Dalton Transactions

ROYAL SOCIETY OF CHEMISTRY

PAPER

View Article Online
View Journal | View Issue

Cite this: *Dalton Trans.*, 2023, **52**, 2293

Synthesis, spectroscopic and structural properties of Sn(II) and Pb(II) triflate complexes with soft phosphine and arsine coordination†

Kelsey R. Cairns, Rhys P. King, Robert D. Bannister, William Levason and Gillian Reid *

Reaction of the divalent $M(OTf)_2$ (M = Sn, Pb; OTf = CF_3SO_3) with soft phosphine and arsine ligands, L, where L = *o*-$C_6H_4(ER_2)_2$ (E = P, R = Me or Ph; E = As, R = Me), $MeC(CH_2ER_2)_3$ (E = P, R = Ph; E = As, R = Me), $PhP(CH_2CH_2PPh_2)_2$ or $P(CH_2CH_2PPh_2)_3$, affords complexes of stoichiometry $M(L)(OTf)_2$ as white powders, which have been characterised *via* elemental analysis, ^{1}H, ^{19}F{^{1}H}, ^{31}P{^{1}H} and ^{119}Sn NMR spectroscopy, with the expected ^{31}P–^{119}Sn and ^{31}P–^{207}Pb couplings clearly evident. The crystal structures of nine of these pnictine complexes are reported, in each case revealing retention of one or both OTf anions, which gives rise to a diverse range of coordination environments including monomers, as well as varying degrees of oligomerisation to form weakly associated (OTf-bridged) dimers, trimers and polymers. ^{19}F{^{1}H} NMR spectra indicate that the OTf is essentially anionic (dissociated) in solution. Anion metathesis of $[M(OTf)_2\{MeC(CH_2PPh_2)_3\}]$ with $Na[BAr^F]$ (BAr^F = B{3,5-$(CF_3)_2C_6H_3$}$_4$) yields the corresponding $[M\{MeC(CH_2PPh_2)_3\}][BAr^F]_2$ salts, the crystal structures of all three (M = Ge, Sn, Pb) reveal pyramidal dications with discrete $[BAr^F]^-$ anions providing charge balance. Density functional theory (DFT) calculations on these $[M\{MeC(CH_2PPh_2)_3\}]^{2+}$ (M = Ge, Sn, Pb) dications using the B3LYP-D3 functional show the presence of a directional lone pair, which is a mixture of valence s and p_z character, with the valence p-orbital character decreasing down group 14. Natural bond orbital (NBO) analysis also shows that the natural charge at the metal centre increases and the charge on the P centre decreases upon going down group 14.

Received 16th November 2022,
Accepted 22nd January 2023

DOI: 10.1039/d2dt03687h

rsc.li/dalton

Introduction

The metallic elements of group 14, germanium, tin and lead have extensive coordination chemistries, for germanium and tin in both the M(II) and M(IV) oxidation states; in contrast very few lead(IV) complexes are known.[1–3] Germanium(IV) halides form mostly six-coordinate complexes with neutral N- and O-donor ligands[1,2] but whilst GeF_4 complexes with phosphine and thioether ligands are well established,[2,4] complexes with arsenic ligands have not been obtained, and $GeCl_4$ and phosphines give redox products $[R_3PCl][GeCl_3]$.[4] There appear to be no crystallographically confirmed complexes of GeI_4.[4] In contrast, tin(IV) halides form many complexes with soft P, As, S and Se ligands; redox chemistry is rarely observed and even SnI_4 forms a significant range of complexes.[1,3,5] Recent work has focussed on attempts to isolate Sn(IV) cations using halide abstraction reagents such as $Na[B\{3,5\text{-}(CF_3)_2C_6H_3\}_4]$ ($Na[BAr^F]$) or $Me_3SiO_3SCF_3$ (TMSOTf).[5] Coordination complexes of Ge(II) were little known for many years, but have received intensive study in the last twenty years.[1,2] Complexes mostly contain halide co-ligands and often a central 3- or 4-coordinate core, with longer interactions to anions in neighbouring molecules in many (but not all) cases producing di-, oligo- or poly-meric structures.[1–3,6] A rich chemistry of Ge(II) cations containing oxa-, aza- or thia-macrocycles,[7] and group 14 tetryliumylidenes has also emerged.[8]

Pnictine chemistry of the M(II) centres is less developed.[3] The $[GeX_2(diphosphine)]$ (diphosphine = $Me_2PCH_2CH_2PMe_2$, $Et_2PCH_2CH_2PEt_2$; X = Cl, Br, I) are discrete four coordinate monomers with near linear GeX_2 units; the $[GeX_2\{o\text{-}C_6H_4(PMe_2)_2\}]$ contain four-coordinate Ge weakly associated into dimers *via* X-bridges.[9] The diarsine complexes include

School of Chemistry, University of Southampton, Southampton SO17 1BJ, UK. E-mail: G.Reid@soton.ac.uk

†Electronic supplementary information (ESI) available: X-ray crystallographic parameters for the structures reported (Table S1), a comparison of the bond lengths and angles determined experimentally (X-ray) with those computed by DFT (Table S2), the multinuclear NMR and IR spectra associated with each of the new compounds described (Fig. S1–S18), and the *x*, *y* and *z* coordinates determined from the DFT calculations. CCDC 2216189–2216200. For ESI and crystallographic data in CIF or other electronic format see DOI: https://doi.org/10.1039/d2dt03687h

$[GeCl\{o\text{-}C_6H_4(AsMe_2)_2\}][GeCl_3]$ and $[GeI_2\{o\text{-}C_6H_4(AsMe_2)_2\}]$, whilst the structure of $[GeX_2\{o\text{-}C_6H_4(PPh_2)_2\}]$ reveals a very asymmetrically coordinated diphosphine, possibly best described as κ^1-coordinated.[9] Halide-free, three-coordinate pyramidal Ge(II) dications, $[Ge(PMe_3)_3][OTf]_2$, $[GeL][OTf]_2$ (L = $MeC(CH_2PPh_2)_3$, $MeC(CH_2AsMe_2)_3$, κ^3-$P(CH_2CH_2PPh_2)_3$), have been described very recently and the electronic structures and bonding probed by DFT calculations.[10]

Much less effort has been devoted to the study of Sn(II) complexes compared to the detailed results available for Sn(IV) compounds.[3] Phosphine complexes of SnF_2 have not been prepared, however, a series of 1 : 1 complexes with $SnCl_2$ was isolated, including $[SnCl_2\{o\text{-}C_6H_4(PMe_2)_2\}]$ and $[SnCl_2\{Me_2PCH_2CH_2PMe_2\}]$ which have a SnP_2Cl_2 core and are weakly associated into dimers *via* chlorine bridges.[11] $[SnCl_2\{o\text{-}C_6H_4(PPh_2)_2\}]$ contained a pyramidal $SnPCl_2$ core with the second phosphino group ~3.29 Å from the tin, and like the germanium analogue is best described as containing a κ^1-diphosphine. The product of reacting $SnCl_2$ and $Ph_2PCH_2CH_2PPh_2$ is $[(SnCl_2)_2\{\mu\text{-}Ph_2PCH_2CH_2PPh_2\}]$, again with a pyramidal $SnPCl_2$ core linked into chains *via* chlorine bridges and with the diphosphine cross-linking the chains.[11] The only reported diarsine complex, $[SnCl\{o\text{-}C_6H_4(AsMe_2)_2\}][SnCl_3]$, like the Ge(II) analogue, is cationic with a polymeric chloride bridged cation.[11] *In situ* ^{31}P and ^{119}Sn NMR data have been obtained from $MeNO_2$ solutions of $Sn[SbF_6]_2$ and various polydentate phosphines including $Ph_2PCH_2CH_2PPh_2$, $PhP(CH_2CH_2PPh_2)_2$, $MeC(CH_2PPh_2)_3$, $\{Ph_2PCH_2CH_2P(Ph)CH_2\}_2$ and $P(CH_2CH_2PPh_2)_3$.[12,13] Although the data mostly indicated three phosphine donors are bound to the tin, none were isolated and no crystallographic data are available.

The coordination chemistry of lead(II) with neutral phosphines is extremely limited.[3] Recent examples of neutral diphosphine complexes are the lead(II) thiolates $[(2,6\text{-}Me_2C_6H_3S)_2Pb]_2\{\mu\text{-}Ph_2P(CH_2)_2PPh_2\}$ and $[(2,6\text{-}Me_2C_6H_3S)_2Pb]_3\{Me_2P(CH_2)_2PMe_2\}$;[14] the latter contains a chain of the three lead centres linked by thiolate bridges, with the $Me_2P(CH_2)_2PMe_2$ chelating to the central Pb. The insoluble, intractable lead dihalides have meant that salts with oxo-anions, $Pb(ClO_4)_2$, $Pb(NO_3)_2$, or fluoroanions have been used.[12,13,15] The reaction of $Pb(NO_3)_2$ with $Me_2P(CH_2)_2PMe_2$, $o\text{-}C_6H_4(PMe_2)_2$ or $Et_2P(CH_2)_2PEt_2$ (L–L) in H_2O/MeCN gave white $[Pb(L\text{–}L)(NO_3)_2]$.[15] The structures of $[Pb\{Me_2P(CH_2)_2PMe_2\}(NO_3)_2]$ and $[Pb\{o\text{-}C_6H_4(PMe_2)_2\}(NO_3)_2]$ reveal chelating diphosphines and κ^2-NO_3 groups occupying one hemisphere about the lead centre, with single oxygen bridges to two further nitrate groups from neighbouring molecules completing a distorted eight-coordinate geometry. $[Pb\{o\text{-}C_6H_4(PMe_2)_2\}(H_2O)(SiF_6)]\cdot H_2O$ has a chelating diphosphine, a coordinated water molecule and a coordinated $[SiF_6]^{2-}$ group, with further Pb–F interactions to neighbouring molecules producing a chain polymer structure.[15] Several polydentate phosphine complexes of $Pb[SbF_6]_2$ (expected 1 : 1 ratio) have also been studied by *in situ* $^{31}P\{^1H\}$ and ^{207}Pb NMR spectroscopy in $MeNO_2$ solution, although none of these complexes were isolated.[12,13]

Here we report a systematic study of the synthesis, X-ray crystal structures and multinuclear NMR spectroscopic data on polydentate pnictine complexes of $Sn[OTf]_2$ and $Pb[OTf]_2$, and compare the results with the Ge(II) analogues, and the reported complexes formed with other anions. The phosphine and arsine ligands used in this work are depicted in Scheme 1.

Experimental

Infrared spectra were recorded as Nujol mulls between CsI plates using a PerkinElmer Spectrum 100 spectrometer over the range 4000–200 cm^{-1}. ^1H, $^{19}F\{^1H\}$, $^{31}P\{^1H\}$ and ^{119}Sn NMR spectra were recorded from CD_3CN solutions using a Bruker AV400 spectrometer and referenced to $SiMe_4$ *via* the residual solvent resonance (^1H), external $CFCl_3$ (^{19}F), 85% H_3PO_4 (^{31}P) and $SnMe_4$ (^{119}Sn), respectively. Duplicate microanalyses were undertaken at Medac Ltd, with the majority of measurements within ±0.4% of the theoretical value. However, in a few cases the values are slightly outside this range, reflecting the recognised inherent variability of microanalytical measurements across different facilities.[16] *n*-Hexane and benzene were dried by distillation from sodium and CH_2Cl_2 and MeCN from CaH_2. All preparations were carried out under anhydrous conditions *via* a dry dinitrogen atmosphere and standard Schlenk and glovebox techniques. Tin(II) triflate and lead(II) triflate, $MeC(CH_2PPh_2)_3$, $PhP(CH_2CH_2PPh_2)_2$, $o\text{-}C_6H_4(PPh_2)_2$ and $P(CH_2CH_2$

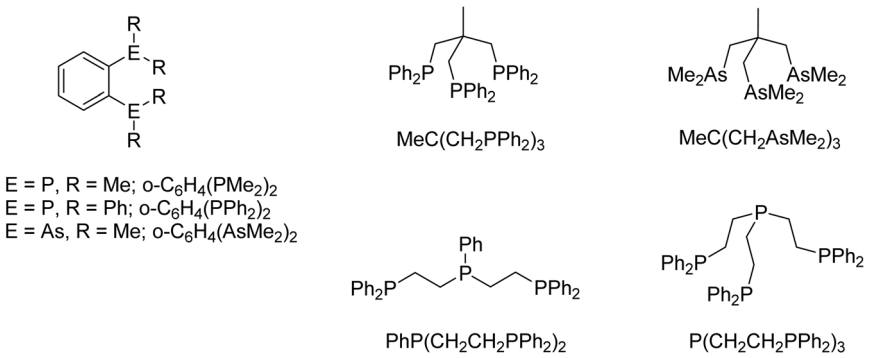

Scheme 1 The pnictine ligands employed in this work.

$PPh_2)_3$ were obtained from Sigma-Aldrich. The other ligands, *o*-$C_6H_4(PMe_2)_2$,[17] *o*-$C_6H_4(AsMe_2)_2$,[18] and $MeC(CH_2AsMe_2)_3$ [18] were prepared by the literature methods. Although formulated as "anhydrous", the IR spectra of the $M(OTf)_2$ typically showed varying amounts of water, which was removed completely by drying *in vacuo* for a few hours before using for the synthesis of the complexes.

X-ray crystallography

Crystals suitable for single crystal X-ray analysis were grown either by layering CH_2Cl_2 solutions with *n*-hexane ($[Sn(OTf)_2\{o\text{-}C_6H_4(PMe_2)_2\}]$ (**1**), $[Sn\{MeC(CH_2PPh_2)_3\}][BAr^F]_2$ (**4**), $[Sn(OTf)\{P(CH_2CH_2PPh_2)_3\}][OTf]$ (**7**), $[Sn(OTf)_2\{o\text{-}C_6H_4(PPh_2)_2\}]$ (**8**), $[Pb(OTf)_2\{o\text{-}C_6H_4(AsMe_2)_2\}]$ (**10**), $[Pb\{MeC(CH_2PPh_2)_3\}][BAr^F]_2$ (**12**), $[Ge\{MeC(CH_2PPh_2)_3\}][BAr^F]_2$ (**15**)), or by vapour diffusion of diethyl ether into MeCN solutions ($[Sn(OTf)_2\{o\text{-}C_6H_4(AsMe_2)_2\}]$ (**2**), $[Sn(OTf)\{PhP(CH_2CH_2PPh_2)_2\}][OTf]$ (**5**), $[Pb(OTf)_2\{o\text{-}C_6H_4(PMe_2)_2\}]$ (**9**), $[Pb(OTf)_2\{MeC(CH_2PPh_2)_3\}]$ (**11**), $[Pb(OTf)\{P(CH_2CH_2PPh_2)_3\}][OTf]$ (**13**)).

Data collections used a Rigaku AFC12 goniometer equipped with an enhanced sensitivity (HG) Saturn724+ detector mounted at the window of an FR-E+ SuperBright molybdenum (λ = 0.71073 Å) rotating anode generator with HF Varimax optics (100 μm focus) with the crystal held at 100 K, or a Rigaku UG2 goniometer equipped with a Rigaku hybrid pixel array detector (Hypix 6000 HE detector) mounted at the window of an FR-E+ SuperBright molybdenum (λ = 0.71073 Å) (or copper, λ = 1.5406 Å, for the three $[BAr^F]$ salts) rotating anode generator with Arc)Sec VHF Varimax confocal mirrors (70 μm focus), with the crystal held at 100 K. Structure solution and refinement were performed using SHELX(S/L)97, SHELX2013, or SHELX-2014/7 *via* Olex.[19] Structure solution and refinement was mostly routine, except for disorder of the OTf and BAr^F anions in some cases, details of which are provided in the relevant cif files. Details of the crystallographic parameters are given in Table 1.

Complex preparations

$[Sn(OTf)_2\{o\text{-}C_6H_4(PMe_2)_2\}]$ (1). $Sn(OTf)_2$ (125 mg, 0.30 mmol) was suspended in benzene (10 mL) before addition of *o*-$C_6H_4(PMe_2)_2$ (60 mg, 0.30 mmol), upon which the majority of solid was taken up into solution which was stirred for 2 h. The remaining particulates were removed by filtration, before the addition of Et_2O (10 mL) which caused precipitation of a white solid, which was collected by filtration and dried *in vacuo*. Yield: 128 mg, 69%. Required for $C_{12}H_{16}F_6O_6P_2S_2Sn$ (615.03): C, 24.43; H, 2.62. Found: C, 24.00; H, 3.04%. ^1H NMR (CD_3CN, 295 K): δ = 7.94–8.01 (m, [2H], Ar–H), 7.78–7.83 (m, [2H], Ar–H), 1.89 (d, $^2J_{P-H}$ = 10.76 Hz, [12H], Me). $^{19}F\{^1H\}$ NMR (298 K, CD_3CN): δ = −78.7 (s, OTf). $^{31}P\{^1H\}$ NMR (298 K, CD_3CN): 14.5 (s, $^1J_{^{117}SnP}$ = 1796 Hz, $^1J_{^{119}SnP}$ = 1878 Hz). ^{119}Sn NMR (298 K, CD_3CN): −689.7 (t, $^1J_{^{119}SnP}$ = 1882 Hz).

$[Sn(OTf)_2\{o\text{-}C_6H_4(AsMe_2)_2\}]$ (2). $Sn(OTf)_2$ (125 mg, 0.30 mmol) was suspended in CH_2Cl_2 (10 mL) before addition of *o*-$C_6H_4(AsMe_2)_2$ (86 mg, 0.30 mmol), upon which the majority of solid dissolved and the solution which was then stirred for 2 h. The remaining particulates were removed by filtration before the addition of *n*-hexane (10 mL) caused precipitation of a white solid, which was collected by filtration and dried *in vacuo*. Yield: 181 mg, 76%. Required for $C_{12}H_{16}As_2F_6O_6S_2Sn{\cdot}CH_2Cl_2$ (787.86) C, 19.82; H, 2.30. Found: C, 19.95; H, 2.49%. ^1H NMR (CD_3CN, 298 K): δ = 7.92–7.97 (m, [2H], Ar–H), 7.75–7.79 (m, [2H], Ar–H), 1.83 (s, [12H], Me). $^{19}F\{^1H\}$ NMR (298 K, CD_3CN): δ = −79.1 (s, OTf). ^{119}Sn NMR (298 K, CD_3CN): not observed; (258 K, CD_3CN): −886.5 (br s).

$[Sn(OTf)_2\{MeC(CH_2PPh_2)_3\}]$ (3). $Sn(OTf)_2$ (83 mg, 0.20 mmol) was partially dissolved in CH_2Cl_2 (10 mL) before addition of $MeC(CH_2PPh_2)_3$ (125 mg, 0.20 mmol), upon which the majority of solid was taken up into solution. The solution was stirred for 2 h. The remaining particulates were removed by filtration, and the solution was concentrated by 50% before addition of *n*-hexane (10 mL) caused precipitation of a white solid which was collected by filtration and dried *in vacuo*. Yield: 177 mg, 81%. Required for $C_{43}H_{39}F_6O_6P_3S_2Sn{\cdot}0.5CH_2Cl_2$ (1083.99): C, 48.20; H, 3.72. Found: C, 47.87; H, 4.26%. ^1H NMR (CD_3CN, 298 K): δ = 7.35–7.50 (m, [18H], Ar–H), 7.20–7.28 (m, [12H], Ar–H), 3.12 (br d, $^2J_{PH}$ = 12 Hz, [6H], CH_2), 2.01 (br s, [3H], Me). $^{19}F\{^1H\}$ NMR (298 K, CD_3CN): δ = −79.2 (s, OTf). $^{31}P\{^1H\}$ (298 K, CD_3CN): δ = −9.4 (s, $^1J_{^{117}SnP}$ = 1189 Hz, $^1J_{^{119}SnP}$ = 1248 Hz). ^{119}Sn NMR (298 K, CD_3CN): δ = −834.0 (q, $^1J_{^{119}SnP}$ = 1242 Hz).

$[Sn\{MeC(CH_2PPh_2)_3\}][BAr^F]_2$ (4). $[Sn(OTf)_2\{MeC(CH_2PPh_2)_3\}]$ (25 mg, 0.023 mmol) was suspended in CH_2Cl_2 (3 mL) before addition of $Na[BAr^F]$ (40 mg, 0.046 mmol) in CH_2Cl_2 (5 mL) and stirred for 30 min. The white precipitate that formed was removed by filtration before the supernatant was concentrated by 50% *in vacuo* and the addition of *n*-hexane, causing precipitation of white solid which was collected by filtration and dried *in vacuo*. Yield: 41 mg, 72%. Required for $C_{105}H_{63}B_2F_{48}P_3Sn$ (2469.80): C, 51.06; H, 2.57. Found: C, 51.21;

Table 1 Comparison of $[M\{MeC(CH_2PPh_2)_3\}][BAr^F]_2$ (M = Ge, Sn, Pb)

	M = Ge (**15**)	M = Sn (**4**)	M = Pb (**12**)
d(M–P)/Å	Ge1–P1 = 2.4239(4) Ge1–P2 = 2.4070(4) Ge1–P3 = 2.4110(5)	Sn1–P1 = 2.6438(4) Sn1–P2 = 2.6194(4) Sn1–P3 = 2.6249(4)	Pb–P1 = 2.7360(5) Pb1–P2 = 2.7092(6) Pb1–P3 = 2.7184(6)
<P–M–P/°	P1–Ge1–P2 = 86.609(14) P1–Ge1–P3 = 85.912(15) P2–Ge1–P3 = 85.412(15)	P1–Sn1–P2 = 82.120(13) P1–Sn1–P3 = 80.761(14) P2–Sn1–P3 = 80.160(14)	P1–Pb1–P2 = 80.594(17) P1–Pb1–P3 = 78.676(17) P2–Pb1–P3 = 77.868(17)

H, 2.50%. ^{1}H NMR (CD_3CN, 298 K): δ = 7.66–7.72 (br m, [16H], Ar–H), 7.65–7.68 (br m, [8H], Ar–H), 7.35–7.42 (br m, [18H] Ar–H) 7.22–7.27 (br m, [12H] Ar–H), 3.11 (br d, $^{2}J_{PH}$ = 12 Hz, [6H], CH_2), 1.99 (br s, [3H], Me). ^{19}F{^{1}H} NMR (298 K, CD_3CN): δ = −63.4 (s, BAr^F). ^{31}P{^{1}H} (298 K, CD_3CN): −8.9 (s, $^{1}J_{SnP}$ = 1246 Hz); (258 K, CD_3CN): −6.0 (s, $^{1}J_{^{119}SnP}$ = 1252 Hz, $^{1}J_{^{117}SnP}$ = 1197 Hz), ^{119}Sn NMR (298 K, CD_3CN): −824.3 (q, $^{1}J_{SnP}$ = 1260 Hz); (258 K, CD_3CN): −843.7 (q, $^{1}J_{SnP}$ = 1251 Hz).

[Sn(OTf){PhP(CH$_2$CH$_2$PPh$_2$)$_2$}][OTf] (5). $Sn(OTf)_2$ (83 mg, 0.20 mmol) was partially dissolved in CH_2Cl_2 (10 mL) before addition of $PhP(CH_2CH_2PPh_2)_2$ (107 mg, 0.20 mmol); the mixture was stirred for 2 h. Particulates were removed by filtration, and the solution was concentrated by 50% *in vacuo* before addition of *n*-hexane (10 mL) caused precipitation of a white solid. This was collected by filtration and dried *in vacuo*. Yield: 141 mg, 71%. Required for $C_{36}H_{33}F_6O_6P_3S_2Sn{\cdot}0.5CH_2Cl_2$ (993.86): C, 44.11; H, 3.45. Found: C, 44.58; H, 2.90%. ^{1}H NMR (CD_3CN, 298 K): δ = 7.78–7.84 (m, [4H], Ar–H), 7.68–7.73 (m, [2H], Ar–H), 7.50–7.64 (m, [9H], Ar–H), 7.31–7.43 (m, [6H], Ar–H), 7.16–7.23 (m, [4H], Ar–H), 3.27–3.45 (br m, [2H], CH_2), 3.00–3.17 (br m, [2H], CH_2), 2.90–3.00 (br m, [2H], CH_2) 2.65–2.78 (br m, [2H], CH_2). ^{19}F{^{1}H} NMR (298 K, CD_3CN): δ = −79.3 (s, OTf). ^{31}P{^{1}H} (298 K, CD_3CN): 36.4 (t, $^{3}J_{PP}$ = 21 Hz, [P], $^{1}J_{^{117}SnP}$ = 1266 Hz, $^{1}J_{^{119}SnP}$ = 1377 Hz), 18.5 (d, $^{3}J_{PP}$ = 21 Hz, [2P], $^{1}J_{^{117}SnP}$ = 1460 Hz, $^{1}J_{^{119}SnP}$ = 1549). ^{119}Sn NMR (298 K, CD_3CN): −834.0 (dt, $^{1}J_{SnP}$ = 1544 Hz, $^{1}J_{SnP}$ = 1386 Hz).

[Sn(OTf)$_2${MeC(CH$_2$AsMe$_2$)$_3$}] (6). $Sn(OTf)_2$ (83 mg, 0.20 mmol) was partially dissolved in CH_2Cl_2 (10 mL) before addition of $MeC(CH_2AsMe_2)_3$ (77 mg, 0.20 mmol), and the mixture then stirred for 2 h. The solution was filtered to remove any remaining solid, concentrated by 50% before addition of *n*-hexane (10 mL) caused precipitation of a white solid which was collected by filtration and dried *in vacuo*. Yield: 77 mg, 43%. Required for $C_{13}H_{27}As_3F_6O_6S_2Sn{\cdot}CH_2Cl_2$ (885.88): C, 18.98; H, 3.30. Found: C, 18.80; H, 3.53%. ^{1}H NMR (CD_3CN, 298 K): δ = 2.15 (s, [6H], CH_2), 1.58 (s, [18H], Me), 1.24 (s, [3H], Me). ^{19}F{^{1}H} NMR (298 K, CD_3CN): δ = −79.2 (s, OTf). ^{119}Sn NMR (298 K, CD_3CN): not observed; (CD_3CN, 258 K): −920 (br).

[Sn(OTf){P(CH$_2$CH$_2$PPh$_2$)$_3$}][OTf] (7). $Sn(OTf)_2$ (83 mg, 0.20 mmol) was partially dissolved in CH_2Cl_2 (10 mL) before addition of $P(CH_2CH_2PPh_2)_3$ (134 mg, 0.20 mmol) and the mixture stirred for 2 h. Any residual solid was removed by filtration, the solution was concentrated by 50% before addition of *n*-hexane (10 mL) caused precipitation of a white solid which was collected by filtration and dried *in vacuo*. Yield: 112 mg, 50%. Required for $C_{44}H_{42}F_6O_6P_4S_2Sn{\cdot}0.5CH_2Cl_2$ (1121.99): C, 47.30; H, 3.84. Found: C, 47.39; H, 3.32%. ^{1}H NMR (CD_3CN, 298 K): δ = 7.38–7.45 (m, [18H], Ar–H), 7.29–7.34 (m, [12H], Ar–H), 2.83–2.94 (br m, [6H], CH_2), 2.63–2.74 (br m, [6H], CH_2). ^{19}F{^{1}H} NMR (298 K, CD_3CN): δ = −79.2 (s, OTf). ^{31}P{^{1}H} (298 K, CD_3CN): 37.8 (br q $^{3}J_{PP}$ = 39 Hz, [P], $^{1}J_{PSn}$ = 1426 Hz), 5.5 (br d, $^{3}J_{PP}$ = 39 Hz, [3P], $^{1}J_{PSn}$ = 711 Hz); (258 K, CD_3CN): 36.3 (br s, [P], $^{1}J_{SnP}$ = 1440 Hz), 3.8 (br s, [3P], $^{1}J_{SnP}$ = 685 Hz); (298 K, CD_2Cl_2): 35.7 (q, $^{3}J_{PP}$ = 35 Hz, [1P], $^{1}J_{SnP}$ = 1103 Hz), 7.34 (d, $^{3}J_{PP}$ = 35 Hz, [3P], $^{1}J_{PSn}$ = 864 Hz); (208 K, CD_2Cl_2): 33.9 (br s, [P], $^{1}J_{SnP}$ = 1123 Hz), 4.59 (br s, [3P], $^{1}J_{PSn}$ = 894 Hz). ^{119}Sn NMR (298 K, CD_3CN): −778.6 (dq, $^{1}J_{^{119}SnP}$ = 1485 Hz, $^{1}J_{^{119}SnP}$ = 720 Hz); (258 K, CD_2CN): −796 (dq, $^{1}J_{^{119}SnP}$ = 732 Hz, $^{1}J_{^{119}SnP}$ = 1477 Hz).

[Sn(OTf)$_2${*o*-C$_6$H$_4$(PPh$_2$)$_2$}] (8). $Sn(OTf)_2$ (104 mg, 0.25 mmol) was partially dissolved in CH_2Cl_2 (10 mL) before addition of o-$C_6H_4(PPh_2)_2$ (112 mg, 0.25 mmol) and then stirred for 2 h. The solution was concentrated by 50% before addition of *n*-hexane (10 mL) caused precipitation of a white solid which was collected by filtration and dried *in vacuo*. Yield: 151 mg, 70%. Required for $C_{32}H_{24}F_6O_6P_2S_2Sn$ (863.31): C, 44.52; H, 2.80. Found: C, 44.20; H, 2.77%. ^{1}H NMR (CD_3CN, 298 K): δ = 7.76–7.79 (br s, [2H], Ar–H), 7.50–7.57 (br m, [6H], Ar–H), 7.46 (br s, [16H], Ar–H). ^{19}F{^{1}H} NMR (298 K, CD_3CN): δ = −79.2 (s, OTf). ^{31}P{^{1}H} (298 K, CD_3CN): 19.8 (br s); (CD_3CN, 258 K): 22.7 (s, $^{1}J_{SnP}$ = 1506 Hz). ^{119}Sn NMR (298 K, CD_3CN): −809 (br s); (CD_3CN, 258 K): −1150 (br t, $^{1}J_{^{119}SnP}$ = 1550 Hz).

[Pb(OTf)$_2${*o*-C$_6$H$_4$(PMe$_2$)$_2$}] (9). $Pb(OTf)_2$ (151 mg, 0.30 mmol) was partially dissolved in CH_2Cl_2 (10 mL) before addition of o-$C_6H_4(PMe_2)_2$ (60 mg, 0.30 mmol), and the solution stirred for 2 h, during which the majority of solid dissolved. The solution was filtered before the addition of Et_2O (10 mL) caused precipitation of a white solid which was collected by filtration and dried *in vacuo*. Yield: 128 mg, 58%. Required for $C_{12}H_{16}F_6O_6P_2PbS_2{\cdot}0.5Et_2O$ (740.58): C, 22.71; H, 2.86. Found: C, 22.56; H, 3.28%. ^{1}H NMR (CD_3CN, 298 K): δ = 7.90–7.95 (m, [2H], Ar–H), 7.73–7.76 (m, [2H], Ar–H), 1.98–2.01 (br m, [12H], Me). ^{19}F{^{1}H} NMR (298 K, CD_3CN): δ = −79.2 (s, OTf). ^{31}P{^{1}H} (298 K, CD_3CN): δ = 74.9 (s, $^{1}J_{PbP}$ = 1777 Hz).

[Pb(OTf)$_2${*o*-C$_6$H$_4$(AsMe$_2$)$_2$}] (10). $Pb(OTf)_2$ (126 mg, 0.25 mmol) was suspended in benzene (10 mL) and o-$C_6H_4(AsMe_2)_2$ (72 mg, 0.25 mmol) and stirring for 2 h. Remaining particulates were removed by filtration before the addition of Et_2O (10 mL) caused precipitation of a white solid which was filtered off and dried *in vacuo*. Yield: 101 mg, 51%. Required for $C_{12}H_{16}As_2F_6O_6PbS_2$ (791.41): C, 18.21; H, 2.04. Found: C, 18.40; H, 2.36%. ^{1}H NMR (CD_3CN, 298 K): δ = 7.83–7.87 (m, [2H], Ar–H), 7.57–7.62 (m, [2H], Ar–H), 1.78 (s, [12H], Me). ^{19}F{^{1}H} NMR (298 K, CD_3CN): δ = −79.1 (s, OTf).

[Pb(OTf)$_2${MeC(CH$_2$PPh$_2$)$_3$}] (11). $Pb(OTf)_2$ (101 mg, 0.20 mmol) was dissolved in CH_3CN (10 mL) before the addition of $MeC(CH_2PPh_2)_3$ (125 mg, 0.20 mmol) and the reaction mixture was stirred for 2 h. Remaining particulates were removed by filtration, the solution was concentrated by 50% causing the precipitation of a white solid which was collected by filtration and dried *in vacuo*. Yield: 115 mg, 51%. Required for $C_{43}H_{39}F_6O_6P_3PbS_2$ (1130.01): C, 45.70; H, 3.48. Found: C, 45.64; H, 3.80%. ^{1}H NMR (CD_3CN, 298 K): δ = 7.33–7.40 (br m, [18H], Ar–H), 7.23–7.29 (m, [12H], Ar–H), 3.04 (br s, [6H], CH_2), 1.65 (br s, [3H], Me). ^{19}F{^{1}H} NMR (298 K, CD_3CN): δ = −79.2 (s, OTf). ^{31}P{^{1}H} (298 K, CD_3CN): δ = 11.6 (s), $^{1}J_{PbP}$ = 1150 (Hz).

[Pb{MeC(CH$_2$PPh$_2$)$_3$}][BAr^F]$_2$ (12). [$Pb(OTf)_2${$MeC(CH_2PPh_2)_3$}] (45 mg, 0.04 mmol) was suspended in CH_2Cl_2 (5 mL) before addition of $Na[BAr^F]$ (71 mg, 0.08 mmol) in CH_2Cl_2 (5 mL) stirred for 30 min. Over this time the solution remained slightly cloudy, but any remaining solid had

changed texture, suggesting formation of a product. Solids were removed by filtration before the solution was concentrated by 50%. Addition of *n*-hexane (10 mL) caused precipitation of a white solid which was collected by filtration and dried *in vacuo*. Yield: 50 mg, 49%. Required for $C_{105}H_{63}B_2F_{48}P_3Pb$ (2558.29): C, 49.30; H, 2.48. Found: C, 49.28; H, 2.01%. ^{1}H NMR (CD_3CN, 298 K): δ = 7.83–7.86 (br m, [16H], Ar–H), 7.67 (br s, [8H], Ar–H), 7.33–7.58 (br m, [6H], Ar–H), 3.45–3.50 (br m, [6H], CH_2), 1.96–1.99 (br m, [3H], Me). ^{19}F{^{1}H} NMR (298 K, CD_3CN): δ = −63.4 (s, BAr^F). ^{31}P{^{1}H} (298 K, CD_3CN): 15.5 (br s); (298 K, CD_3NO_2): 15.8 (s), $^1J_{PbP}$ = 1777 Hz.

[Pb(OTf){P(CH$_2$CH$_2$PPh$_2$)$_3$}][OTf] (13). $Pb(OTf)_2$ (101 mg, 0.20 mmol) was added to MeCN (10 mL) followed by $P(CH_2CH_2PPh_2)_3$ (134 mg, 0.20 mmol), upon which the majority of solid dissolved; the mixture was stirred for 2 h. Remaining particulates were removed by filtration, and the solution was concentrated to 50% volume before the addition of *n*-hexane (10 mL), which caused precipitation of a white solid. This was collected by filtration and dried *in vacuo*. Yield: 89 mg, 38%. Crystals were grown from CH_2Cl_2 solution. Required for $C_{44}H_{39}F_6O_6P_4PbS_2{\cdot}0.3CH_2Cl_2$ (1172.99): C, 44.94; H, 3.60. Found: C, 44.42; H, 3.96%. ^{1}H NMR (CD_3CN, 298 K): δ = 7.37–7.48 (m, [18H] Ar–H), 7.30–7.34 (m, [12H], Ar–H), 2.79–2.90 (br m, [6H], CH_2), 2.58–2.70 (br m, [6H], CH_2). ^{19}F{^{1}H} NMR (298 K, CD_3CN): δ = −79.2 (s, OTf). ^{31}P{^{1}H} (298 K, CD_3CN): δ = 77.5 (q, $^1J_{PbP}$ = 437 Hz, $^3J_{PP}$ = 44 Hz, [P]), 26.1 (d, $^1J_{PbP}$ = 1870, $^3J_{PP}$ = 44 Hz, [3P]).

[Pb(OTf)$_2${MeC(CH$_2$AsMe$_2$)$_3$}] (14). $Pb(OTf)_2$ (101 mg, 0.20 mmol) was partially dissolved in CH_3CN (10 mL) before addition of $MeC(CH_2AsMe_2)_3$ (125 mg, 0.20 mmol), and the mixture then stirred for 2 h. The solution was concentrated by 50% before addition of Et_2O (10 mL) caused precipitation of a white solid over 10 min of stirring and was then collected by filtration and dried *in vacuo*. Yield: 41 mg, 23%. Required for $C_{13}H_{27}As_3F_6O_6PbS_2$ (889.43): C, 17.55; H, 3.06. Found: C, 17.11; H, 3.09%. ^{1}H NMR (CD_3CN, 298 K): δ = 2.21 (s, [6H], CH_2), 1.61 (s, [18H], Me), 1.16 (s, [3H], Me). ^{19}F{^{1}H} NMR (298 K, CD_3CN): δ = −79.3 (s, OTf).

[Ge{MeC(CH$_2$PPh$_2$)$_3$}][BAr^F]$_2$ (15). [Ge{MeC(CH$_2$PPh$_2$)$_3$}][OTf]$_2$ [9] (0.050 g, 0.05 mmol) was suspended in CH_2Cl_2 (1 mL), Na[BAr^F] (0.089 g, 0.10 mmol) added, the solution was stirred for ∼10 min, forming a colourless solution with a small amount of precipitate (NaOTf). The supernatant was filtered away from the solid and layered with *n*-hexane (2 mL). After 24 h colourless crystals formed which were isolated by filtration and dried *in vacuo*. The crystals were suitable for single crystal X-ray diffraction. Yield: 0.068 mg, 56%. Required for $C_{105}H_{63}B_2F_{48}P_3Ge$ (2423.59): C, 52.03; H, 2.62. Found: C, 52.26; H, 2.84%. ^{1}H NMR (298 K, CD_2Cl_2): δ = 7.71–7.75 (m, [16H], Ar–H), 7.55–7.57 (s, [8H], Ar) 7.38–7.43 (m, [6H], Ar–H), 7.20–7.25 (m, [24H], Ar–H), 3.02–3.07 (m, [6H], CH_2), 2.12–2.18 (q, [3H], $^4J_{PH}$ = 4.0 Hz, Me). ^{19}F{^{1}H} NMR (298 K, CD_2Cl_2): δ = −62.8 (s, BAr^F). ^{31}P{^{1}H} NMR (298 K, CD_2Cl_2): δ = −4.34 (s).

DFT calculations

The electronic structures of the set of dications, [M{MeC(CH$_2$PPh$_2$)$_3$}]$^{2+}$ (M = Ge, Sn, Pb; (**4**), (**12**), (**15**)), were investigated using DFT calculations using the Gaussian 16 W software package.[20] The density functional used was B3LYP-D3,[21] with the basis set 6-311G(d) for H, C, P and Ge atoms[22] and the lanl2dz basis set for the Sn and Pb atoms.[23] For M = Ge and Sn the initial geometries were taken from their crystal structures, while for M = Pb the initial geometry chosen was from the optimised structure of M = Sn with the tin atom replaced for lead. Calculations for all structures converged with no imaginary frequencies. The calculated structures were found to be in good agreement with the crystallographically-derived metrics (see Table S2†).

Results and discussion

The triflate complexes were prepared in good yield by reaction of a suspension of M[OTf]$_2$ (M = Sn, Pb) in an organic solvent with a solution of the di-, tri- or tetra-pnictine ligand in a 1 : 1 molar ratio (Scheme 2). The BAr^F salts were prepared from the triflate complexes by metathesis with Na[BAr^F] in CH_2Cl_2. The complexes were white powders or colourless crystals with a 1 : 1 M : pnictine ratio confirmed by microanalysis, with the solids being stable over several weeks in dry air and in daylight. In solution some slow degradation hydrolysis is observed *via* NMR spectroscopy after 2–3 h. The related literature (Introduction) suggests that many of the complexes are likely to be oligomeric,[3,9,11,15] and only very limited data on the solids is provided by spectroscopy. We therefore determined the X-ray crystal structures of six of the tin and five of the lead complexes and discuss these first. The multinuclear NMR spectroscopic behaviour will then be considered to explore the solution speciation.

X-ray crystal structures

The structure of [Sn(OTf)$_2${*o*-C$_6$H$_4$(PMe$_2$)$_2$}] (**1**) shows a distorted four-coordinate tin core, which could be described as tetragonal pyramidal or as a trigonal bipyramid with a vacant equatorial vertex (Fig. 1(a)). The Sn–P distances are not significantly different from those in [SnCl$_2${*o*-C$_6$H$_4$(PMe$_2$)$_2$}][11] and the two coordinated triflates have O–Sn–O angles of 144.36(14)°. However, while [SnCl$_2${*o*-C$_6$H$_4$(PMe$_2$)$_2$}][11] forms a dimeric unit *via* chloride bridges, in the triflate complex two triflates from neighbouring molecules also coordinate weakly (Sn⋯O ∼3.0 Å) to form a trimeric assembly (Fig. 1b), well within the sum of the van der Waals radii for Sn + O (3.69 Å).[24] Note that we have considered M⋯O distances up to 0.3 Å below the sum of the van der Waals distances to be long, weak interactions.

In the Ph-substituted diphosphine analogue, [Sn(OTf)$_2${*o*-C$_6$H$_4$(PPh$_2$)$_2$}] (**8**), the two *d*(Sn–P) are quite similar (2.7179(10), 2.8186(11) Å), which contrasts with the essentially κ^1-coordination of the diphosphine present in the reported tin(II) chloride analogue, [SnCl$_2${*o*-C$_6$H$_4$(PPh$_2$)$_2$}], where *d*(Sn–P) = 2.8293(9) and 3.285(1) Å.[11] The [Sn(OTf)$_2${*o*-C$_6$H$_4$(PPh$_2$)$_2$}]

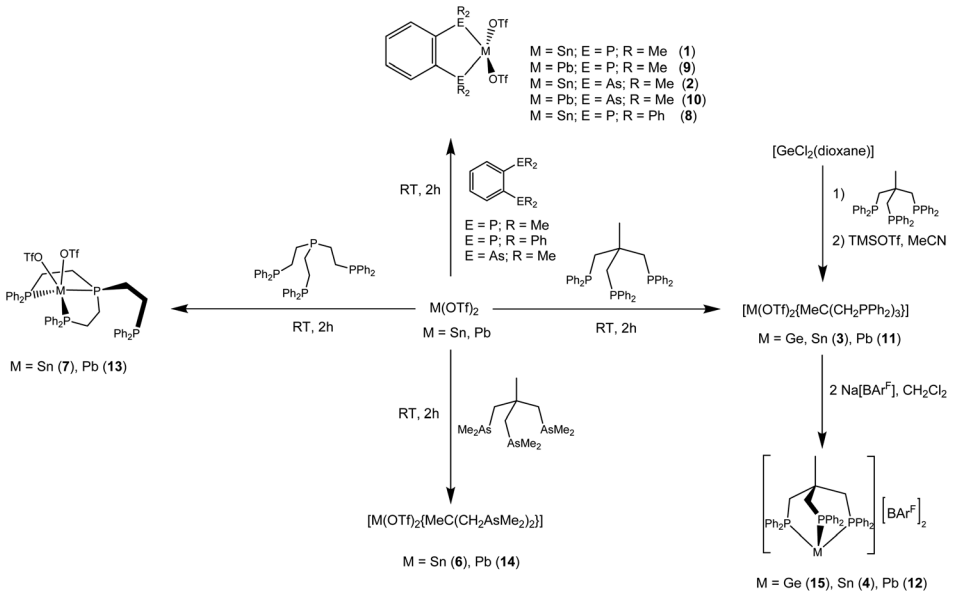

Scheme 2 Synthesis routes to the pnictine complexes reported in this work.

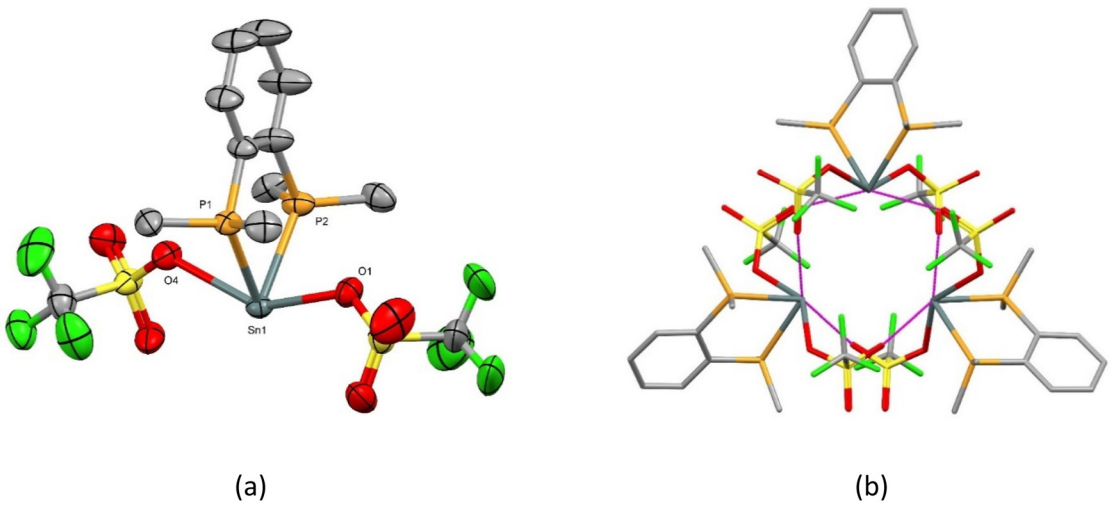

Fig. 1 (a) View of the structure of the Sn1-centred $[Sn(OTf)_2\{o\text{-}C_6H_4(PMe_2)_2\}]$ (**1**) moiety in the asymmetric unit showing the atom numbering scheme (there is a similar, but crystallographically independent Sn2-centred moiety in the asymmetric unit). H atoms are omitted for clarity. Ellipsoids are drawn at the 50% probability level. There are two slightly different molecules in the cell, only one is shown. Selected bond lengths (Å) and angles (°) for the Sn1-centred unit: Sn1–P1 = 2.6723(14), Sn1–P2 = 2.6682(15), Sn1–O1 = 2.346(4), Sn1–O4 = 2.527(4), Sn1···O3′ = 2.967(4), Sn1···O8 = 3.002(4), P2–Sn1–P1 = 75.85(5), O1–Sn1–P1 = 77.890(11), O1–Sn1–P2 = 79.14(11), O1–Sn1–O4 = 144.36(14), O4–Sn1–P1 = 72.74(9), O4–Sn1–P2 = 74.50(11); (b) the weakly associated trimeric unit.

molecules in (**8**) form weakly associated dimers containing one κ^1-coordinated OTf per tin centre (Sn1–O1 = 2.472(3) Å) and two bridging triflates with longer (weaker) Sn···OTf contacts (Fig. 2).

The core structure of the diarsine complex, $[Sn(OTf)_2\{o\text{-}C_6H_4(AsMe_2)_2\}]$ (**2**) (Fig. 3(a)) is similar to that of its diphosphine analogue, $[Sn(OTf)_2\{o\text{-}C_6H_4(PMe_2)_2\}]$ (**1**), although, unlike the phosphorus analogue, the triflates are symmetrically bound (due to crystallographic symmetry). This complex also oligomerises *via* long Sn···OTf contacts (Fig. 3(b)).

The structure of $[Sn\{MeC(CH_2PPh_2)_3\}][BAr^F]_2$ (**4**) (Fig. 4), as expected, shows no cation–anion interaction due to the diffuse nature of the large BAr^F anion. In this case the tin is in a P_3 trigonal pyramidal geometry, with all three Sn–P bond distances in the range 2.6194(4)–2.6438(4) Å, *i.e.* rather shorter than in the complexes described above with coordinated triflate. This probably reflects the lower coordination number and higher cationic charge.

The complexes $[Sn(OTf)\{PhP(CH_2CH_2PPh_2)_2\}][OTf]$ (**5**) and $[Sn(OTf)\{P(CH_2CH_2PPh_2)_3\}][OTf]$ (**7**) involve coordination to Sn

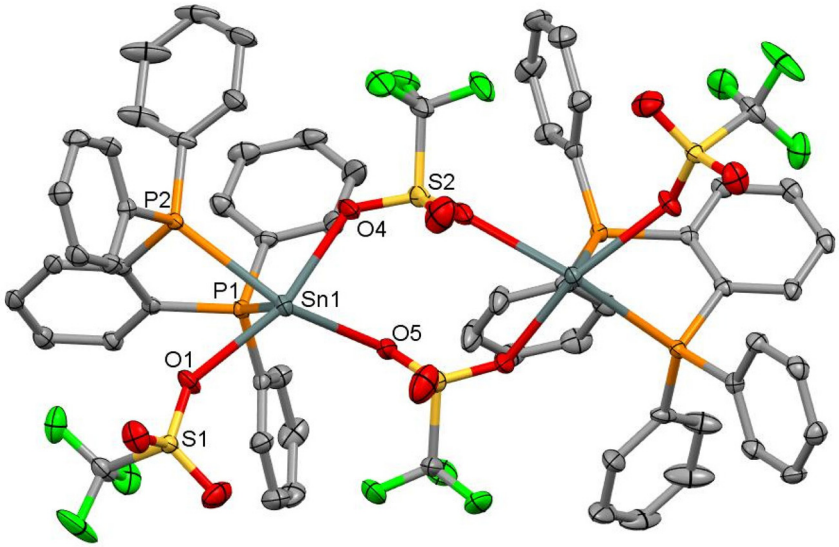

Fig. 2 View of the OTf-bridged dimer present in $[Sn(OTf)_2\{o\text{-}C_6H_4(PPh_2)_2\}]$ (**8**) showing the atom numbering scheme. H atoms and CH_2Cl_2 solvent are omitted for clarity. Ellipsoids are drawn at the 50% probability level. Selected bond lengths (Å) and angles: Sn1–P1 = 2.7179(10), Sn1–P2 = 2.8186 (11), Sn1–O1 = 2.472(3), Sn1–O4 = 2.394(3), Sn1···O5 = 2.751(3), Sn1···O6 = 3.318(4), P1–Sn1–P2 = 69.80(3), O1–Sn1–P1 = 76.66(7), O1–Sn1–P2 = 76.94(8), O4–Sn1–P1 = 91.53(10), O4–Sn1–P2 = 85.14(8), O4–Sn1–O1 = 161.06(11).

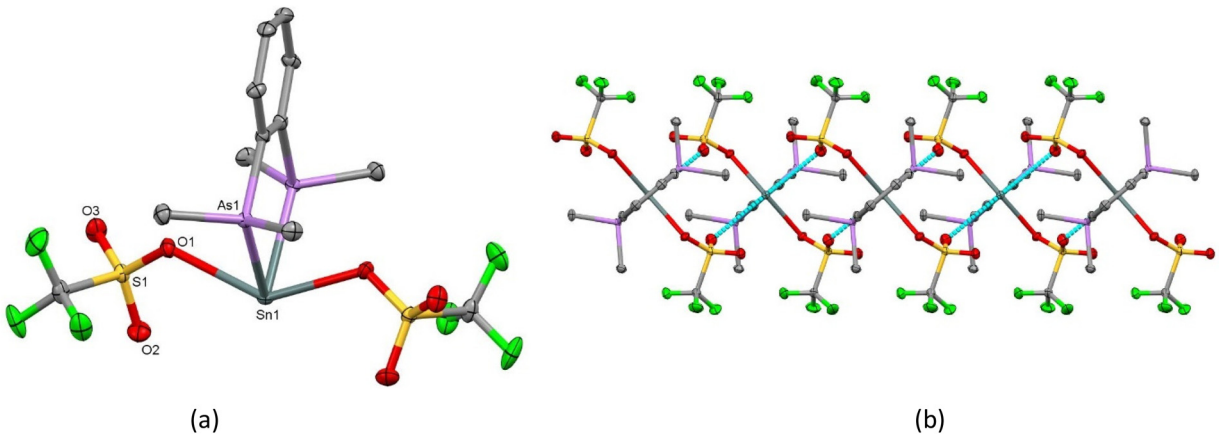

Fig. 3 (a) View of core of $[Sn(OTf)_2\{o\text{-}C_6H_4(AsMe_2)_2\}]$ (**2**) showing the atom numbering scheme. H atoms are omitted for clarity. Ellipsoids are drawn at the 50% probability level. Selected bond lengths (Å) and angles (°): Sn1–As1 = 2.7585(2), Sn1–O1 = 2.4438(12), Sn1··· O2 = 3.0094(14), O1–Sn1–O1 = 137.76(6), O1–Sn1–As1 = 73.75(3), As1–Sn1–As1 = 76.755(8); (b) part of the polymeric chain with bridging OTf groups viewed down the *b*-axis.

(II) *via* a P_3O donor set, with a further long, weak interaction to the second triflate completing a very distorted five-coordinate geometry (Fig. 5). The Sn–P bond lengths range from 2.6800 (12)–2.8412(7) Å, are longer than in the tripodal dication in $[Sn\{MeC(CH_2PPh_2)_3\}][BAr^F]_2$ (**4**), discussed above and the fourth phosphine group (–PPh_2) in $[Sn(OTf)\{P(CH_2CH_2PPh_2)_3\}][OTf]$ (**7**) points away from the tin and is not involved in coordination. The Ge(II) analogue adopts a three-coordinate pyramidal structure, with the triflate anions not coordinated.[10] In both of these structures, as expected, the P–Sn–P angles involved in the five-membered chelate rings are substantially smaller than the much less constrained P1–Sn–P3 angles.

Moving now to the crystal structures determined for the Pb(II) complexes, the four-coordinate core geometry in $[Pb(OTf)_2\{o\text{-}C_6H_4(PMe_2)_2\}]$ (**9**) (Fig. 6(a)) is very similar to that in the corresponding tin complex (above), and the coordination through bridging triflate groups (longer Pb···OTf contacts) from neighbouring molecules results in a zig-zag polymer chain with (effectively) six-coordination about the lead (Fig. 6(b)) (there is a further OTf group 3.26 Å away from the Pb centre, but this distance is only 0.28 Å within the sum of the van der Waals radii for Pb + O, 3.54 Å,[24] and therefore we do not consider this to be a significant interaction).

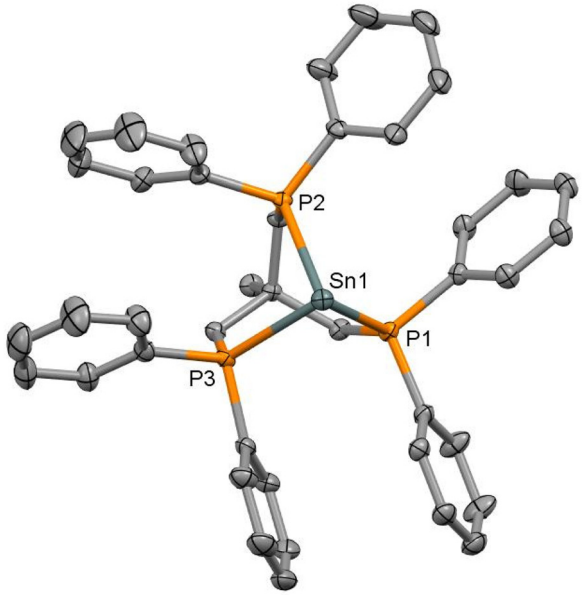

Fig. 4 View of the cation in $[Sn\{MeC(CH_2PPh_2)_3\}][BAr^F]_2$ (**4**) showing the atom numbering scheme. H atoms are omitted for clarity. Ellipsoids are drawn at the 50% probability level. Selected bond lengths (Å) and angles: Sn1–P1 = 2.6438(4), Sn1–P2 = 2.6194(4), Sn1–P3 = 2.6249(4), P1–Sn1–P2 = 82.120(13), P1–Sn1–P3 = 80.761(14), P2–Sn1–P3 = 80.160(14).

The lead(II) diarsine complex, $[Pb(OTf)_2\{o\text{-}C_6H_4(AsMe_2)_2\}]$ (**10**), has core $PbAs_2O_2$ coordination and also forms a chain polymer *via* weakly bridging OTf groups, with overall six-coordination at Pb(II) and with two very similar Pb–As distances (Fig. 7).

The crystal structure of $[Pb(OTf)\{P(CH_2CH_2PPh_2)_3\}][OTf]$ (**13**) is isomorphous with the tin analogue above, showing P_3O_2 coordination, with the third pendant $-PPh_2$ group remaining uncoordinated, and with the P1–Pb–P3 angle rather more open than those involving the constrained five-membered chelate rings (Fig. 8).

The structure of the lead triflate complex with the tripodal triphosphine, $[Pb(OTf)_2\{MeC(CH_2PPh_2)_3\}]$ (**11**), reveals a dimer with three bridging (and one ionic) triflates (Fig. 9), and therefore is better formulated as $[\{Pb\{MeC(CH_2PPh_2)_3\}\}_2(\mu\text{-}OTf)_3][OTf]$. In contrast, the corresponding BAr^F salt, $[Pb\{MeC(CH_2PPh_2)_3\}][BAr^F]_2$ (**12**), shows a discrete three-coordinate cation (Fig. 10(a)). Comparison of the $[BAr^F]$ and OTf structures shows longer Pb–P bonds in the latter, attributable to the higher coordination number. The P–Pb–P bond angles of the triflate bridged species ranged from 71.678(13)–77.348(13), significantly more acute than those seen in the BAr^F salt (77.868(17)–80.594(17)°).

We also prepared the lighter group 14 congener (M = Ge), $[Ge\{MeC(CH_2PPh_2)_3\}][BAr^F]_2$ (**15**), and determined its structure (Fig. 10(b)). The three salts, $[M\{MeC(CH_2PPh_2)_3\}][BAr^F]_2$ (M = Ge, Sn, Pb), are isomorphous ($P\bar{1}$). As indicated in the Introduction, it is very unusual to find three isomorphous structures for pnictine complexes of these three elements, and as can be seen from Table 1, the M–P bond distances increase in the order Ge < Sn < Pb, and the P–M–P angles decrease in

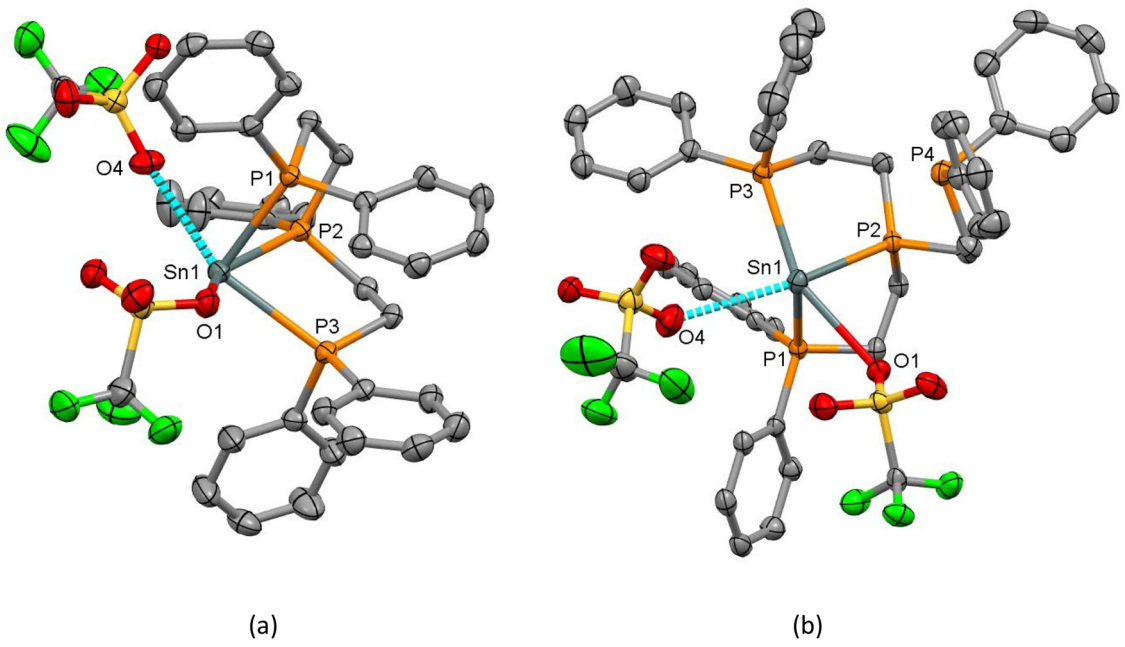

Fig. 5 (a) View of the structure of $[Sn(OTf)\{PhP(CH_2CH_2PPh_2)_2\}][OTf]$ (**5**) showing the atom numbering scheme. H atoms are omitted for clarity. Ellipsoids are drawn at the 50% probability level. Selected bond lengths (Å) and angles (°): Sn1–P1 = 2.6800(12), Sn1–P2 = 2.7655(12), Sn1–P3 = 2.7627(12), Sn–O1 = 2.623(4), Sn···O4 = 2.821(4), P1–Sn1–P2 = 74.52(4), P1–Sn1–P3 = 90.23(4), P2–Sn1–P3 = 72.35(4); (b) view of the structure of $[Sn(OTf)\{P(CH_2CH_2PPh_2)_3\}][OTf]$ (**7**) showing the atom numbering scheme. Selected bond lengths (Å) and angles (°): Sn1–P1 = 2.7085(7), Sn1–P2 = 2.7055(7), Sn1–P3 = 2.8412(7), Sn1–O1 = 2.698(2), Sn1···O4 = 2.968(3), P1–Sn1–P2 = 74.31(2), P1–Sn1–P3 = 96.68(2), P2–Sn1–P3 = 72.82(2).

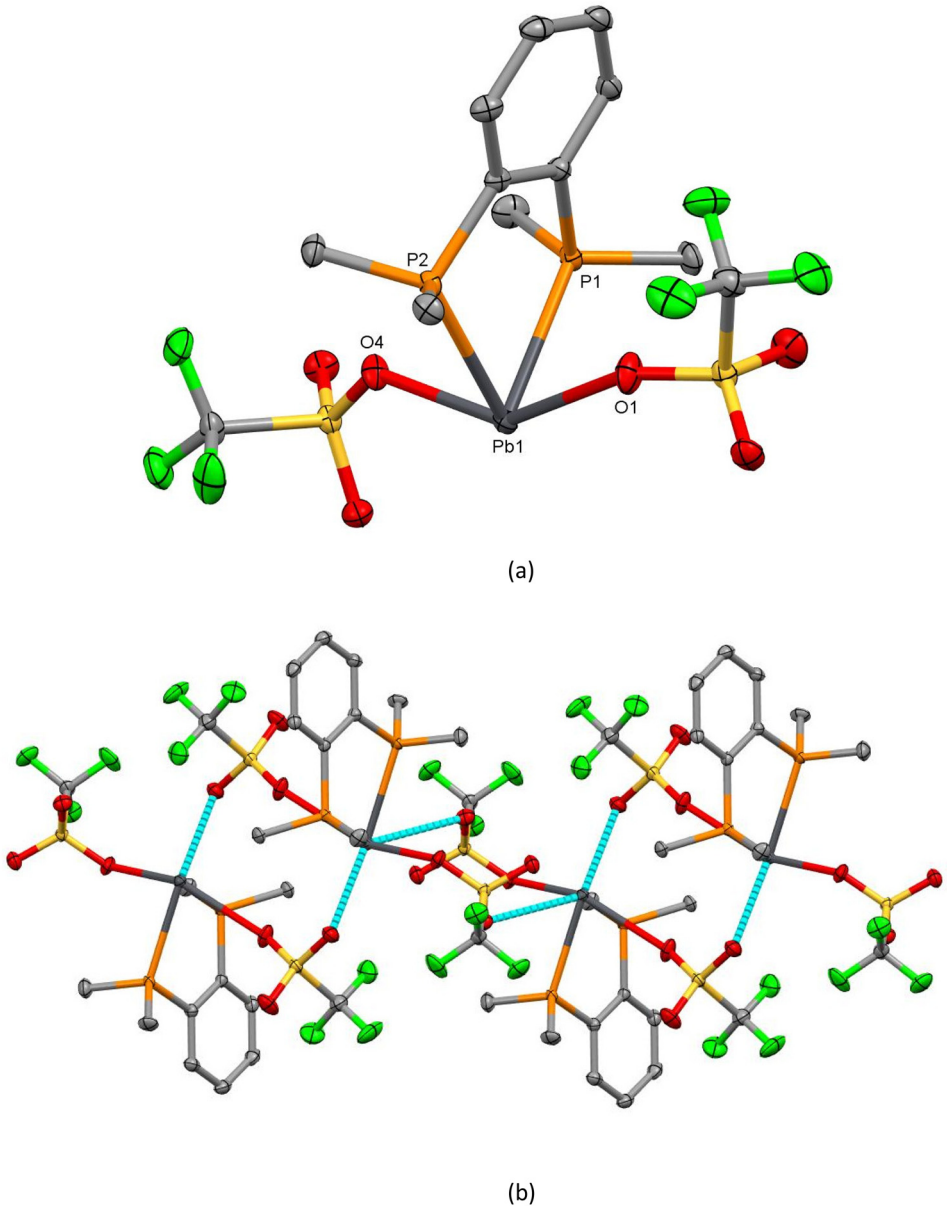

Fig. 6 (a) View of the of $[Pb(OTf)_2\{o\text{-}C_6H_4(PMe_2)_2\}]$ (**9**) core showing the atom numbering scheme. H atoms are omitted for clarity. Ellipsoids are drawn at the 50% probability level. Selected bond lengths (Å) and angles (°): Pb1–P1 = 2.7623(6), Pb1–P2 = 2.7581(6), Pb1–O1 = 2.6740(19), Pb1–O4 = 2.4504(19), Pb1···O3 = 2.9394(19), Pb1···O5 = 3.0193(19), P2–Pb1–P2 = 72.473(18), O1–Pb1–P1 = 76.99(5), O1–Pb1–P2 = 72.28(5), O4–Pb1–P1 = 79.60(5), O4–Pb1–P2 = 77.71(4), O4–Pb1–O1 = 146.26(7); (b) the OTf-bridged chain structure present in $[Pb(OTf)_2\{o\text{-}C_6H_4(PMe_2)_2\}]$.

the same order. The increase in d(M–P) down group 14 is consistent with the increase in the covalent radii.[25]

Spectroscopic data

To probe the solution speciation, multinuclear NMR spectra (^{1}H, ^{19}F$\{^1$H$\}$, ^{31}P$\{^1$H$\}$ and ^{119}Sn) were recorded, usually from CD_3CN or CD_3NO_2, or, if solubility permitted, from CD_2Cl_2 solutions. The ^{1}H spectra (see Experimental and ESI†) were consistent with the coordinated pnictine, but were otherwise rather uninformative. The ^{19}F$\{^1$H$\}$ data of the triflate complexes each show a sharp singlet at *ca.* −79 ppm, assigned to ionic triflate, indicating that the $[OTf]^-$ groups are at best weakly associated or exchanging in solution. The ^{31}P$\{^1$H$\}$ and ^{119}Sn spectra are much more informative and key data are summarised in Table 2, with representative examples shown in Fig. 11 and 12, (full data are in the Experimental section and the ESI†). Table 2 also summarises data on related $[M(phosphine)][SbF_6]_2$ taken from the *in situ* studies by Dean and co-workers.[12,13] In some cases three examples with different anions are known for a specific phosphine, for example $[Sn\{MeC(CH_2PPh_2)_3\}]Y_2$ with Y^- = $[BAr^F]^-$, $[SbF_6]^-$ and $[OTf]^-$. The ^{119}Sn chemical shifts for these are very similar, indicating the phosphine plays the dominant role. The ^{31}P$\{^1$H$\}$ NMR chemical shifts

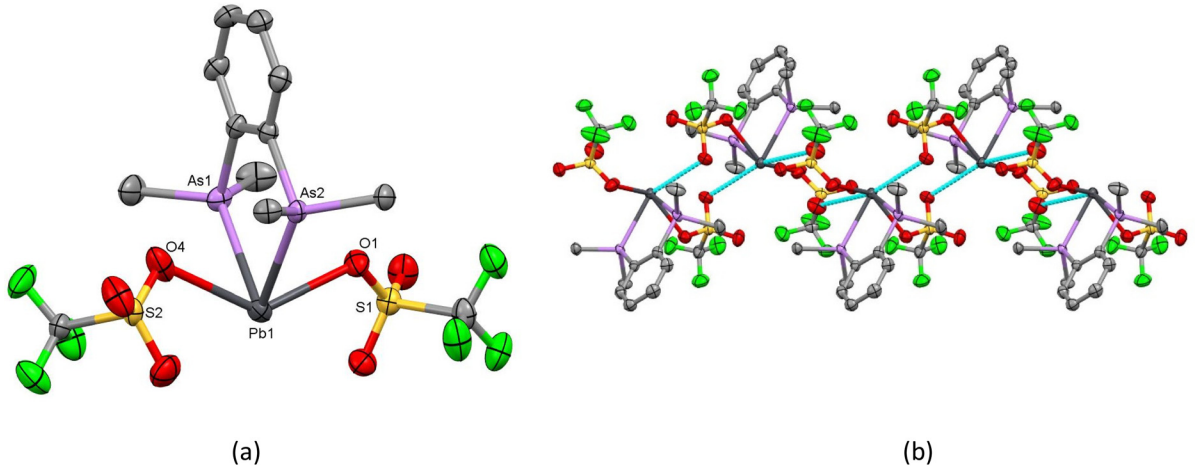

Fig. 7 (a) View of the of $[Pb(OTf)_2\{o\text{-}C_6H_4(AsMe_2)_2\}]$ (**10**) core showing the atom numbering scheme. H atoms are omitted for clarity. Ellipsoids are drawn at the 50% probability level. Selected bond lengths (Å) and angles (°): Pb1–As1 = 2.8675(6), Pb1–As2 = 2.8752(6), Pb1–O1 = 2.539(4), Pb1–O4 = 2.712(5), Pb1···O4 = 2.712(5), Pb1···O5 = 2.972(5), As1–Pb1–As2 = 73.297(16), O4–Pb1–As1 = 69.56(9), O4–Pb1–As2 = 69.84(10), O1–Pb1–O4 = 133.97(13), O1–Pb1–As1 = 74.98(10), O1–Pb1–As2 = 72.57(9); (b) view of the polymeric chain in $[Pb(OTf)_2\{o\text{-}C_6H_4(AsMe_2)_2\}]$.

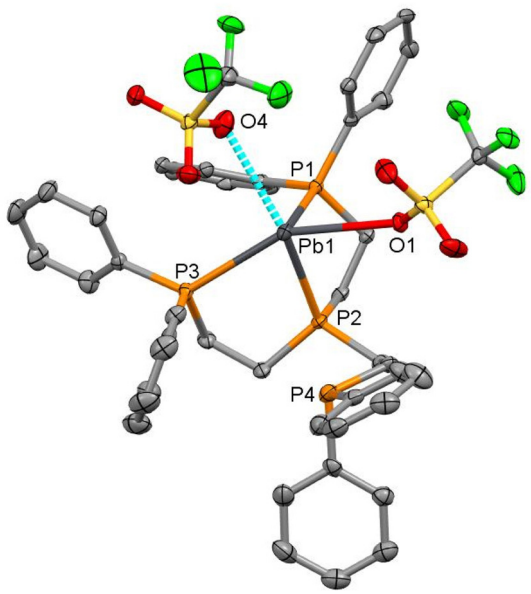

Fig. 8 View of the structure of $[Pb(OTf)\{P(CH_2CH_2PPh_2)_3\}][OTf]$ (**13**) showing the atom numbering scheme. H atoms are omitted for clarity. Ellipsoids are drawn at the 50% probability level. Selected bond lengths (Å) and angles (°): Pb1–P1 = 2.7771(8), Pb1–P2 = 2.8021(7), Pb1–P3 = 2.9185(7), Pb1–O1 = 2.7514(19), Pb···O4 = 2.951(2), P1–Pb1–P2 = 72.95 (2), P1–Pb1–P3 = 96.20(2), P2–Pb1–P3 = 70.72(2), O1–Pb1–P1 = 71.18 (5), O1–Pb1–P2 = 75.99(4), O1–Pb1–P3 = 146.61(4).

and the coupling constants are much more variable, possibly reflecting the different solvents in some cases, and probably some interaction of the anions or phosphine exchange. While coordination by $[SbF_6]^-$ is viewed as rare,[26] examples are known in the solid state, and coordinated triflate is well known.

Also notable are the NMR data on the $[Sn\{P(CH_2CH_2PPh_2)_3\}]^{2+}$ cation incorporating the tripodal tetraphosphine, whose ^{31}P and ^{119}Sn NMR spectra are consistent with all three PPh_2 groups appearing to interact with the tin, suggesting tetradentate coordination on average in solution. This is in contrast to the κ^3-phosphine coordination found in the solid state structure of $[Sn(OTf)\{P(CH_2CH_2PPh_2)_3\}][OTf]$ (7) described above, in which the one pendant arm remains free. Upon cooling the solution of this complex to 258 K (MeCN), the lines broaden, but do not split, probably indicating fast exchange between coordinated and free pendant $-PPh_2$ groups, which is not frozen out at the lower temperature.

The tin-arsine complexes did not exhibit ^{119}Sn NMR resonances at room temperature, but broad resonances appear upon cooling the solutions to 258 K, with chemical shifts somewhat more negative than the analogous phosphine complexes.

The lead phosphine species incorporating $[SbF_6]^-$ anions previously reported by Dean *et al.* were generated *in situ*, but never isolated.[12,13] These solutions did exhibit ^{207}Pb NMR resonances, however, although the $[OTf]^-$ and $[BAr^F]^-$ complexes isolated in the present study show clear ^{207}Pb lead satellites in their $^{31}P\{^1H\}$ NMR spectra, which sharpen at low temperature, we were unable to observe ^{207}Pb NMR resonances in a similar chemical shift range to those in the reported work, either at room temperature or upon cooling in MeCN (258 K). For the triflate complexes it seems most likely that this is a result of rapid reversible coordination of the triflate ions (consistent with coordination of OTf groups in the crystal structures of several examples described above). The $^{31}P\{^1H\}$ NMR data above also revealed fast phosphine exchange in solutions of some of the Sn(II) and Pb(II) complexes, and this may explain the absence of a ^{207}Pb NMR resonance in the $[Pb\{MeC(CH_2PPh_2)_3\}][BAr^F]_2$ (**12**) complex, where the low temperature limiting spectrum may not have been reached at 258 K, which is the low temperature limit for $MeNO_2$.

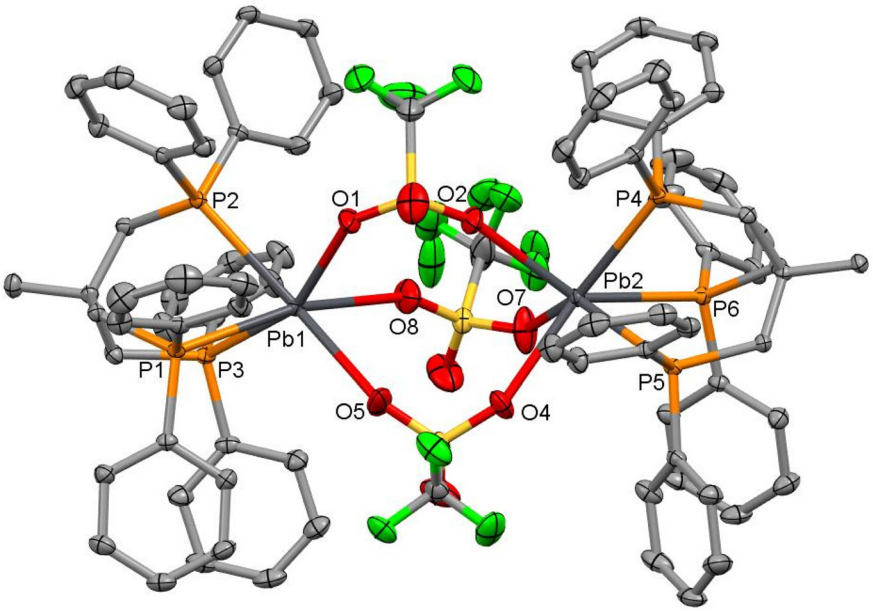

Fig. 9 View of the structure of the cation in $[\{Pb\{MeC(CH_2PPh_2)_3\}_2(\mu\text{-}OTf)_3\}][OTf]$ (**11**) showing the atom numbering scheme. H atoms are omitted for clarity. Ellipsoids are drawn at the 50% probability level. Selected bond lengths (Å) and angles (°): Pb1–P1 = 2.8277(4), Pb1–P2 = 2.8844(4), Pb1–P3 = 2.9261(5), Pb1–O1 = 2.6542(15), Pb1–O5 = 2.7722(15), Pb1···O8 = 2.8398(15), Pb2–P4 = 2.9075(5), Pb2–P5 = 2.8441(5), Pb2–P6 = 2.9158(5), Pb2–O2 = 2.7889(14), Pb2–O4 = 2.6707(14), Pb2···O7 = 2.7375(17), P1–Pb1–P3 = 72.800(13), P2–Pb1–P3 = 77.348(13), P1–Pb1–P2 = 71.678(13).

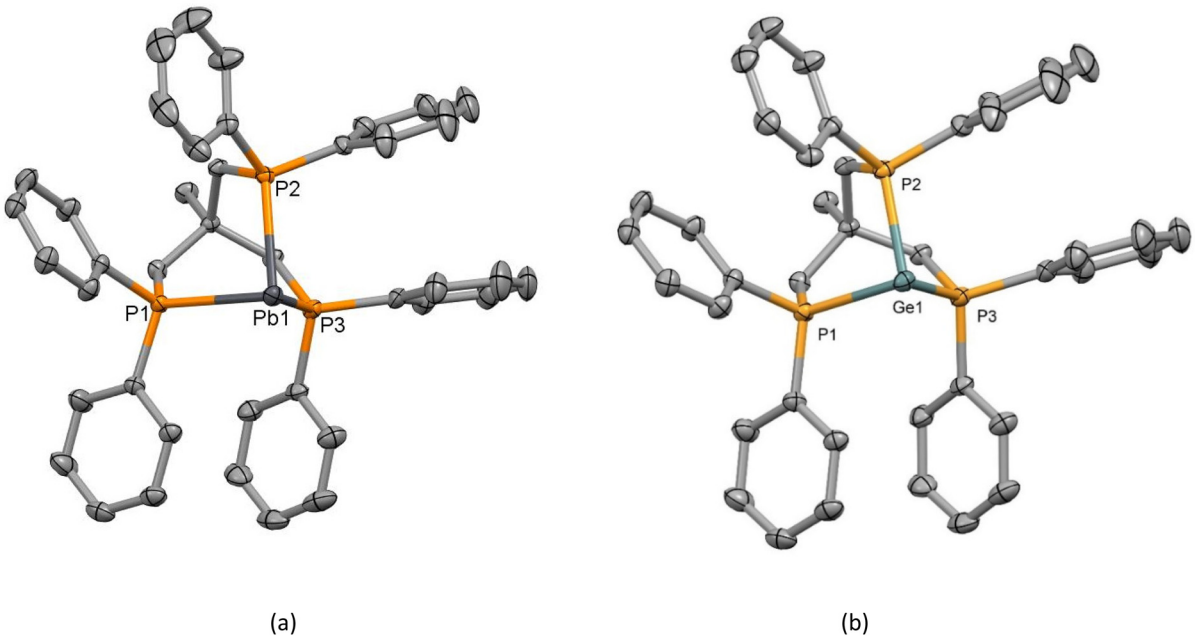

(a) (b)

Fig. 10 (a) View of the cation in $[Pb\{MeC(CH_2PPh_2)_3\}][BAr^F]_2$ (**12**) showing the atom numbering scheme. H atoms are omitted for clarity. Ellipsoids are drawn at the 50% probability level. Selected bond lengths (Å) and angles (°): Pb–P1 = 2.7360(5), Pb1–P2 = 2.7092(6), Pb1–P3 = 2.7184(6), P1–Pb1–P2 = 80.594(17), P1–Pb1–P3 = 78.676(17), P2–Pb1–P3 = 77.868(17); (b) view of the cation in $[Ge\{MeC(CH_2PPh_2)_3\}][BAr^F]_2$ (**15**) showing the atom numbering scheme. H atoms are omitted for clarity. Ellipsoids are drawn at the 50% probability level. Selected bond lengths (Å) and angles: Ge1–P1 = 2.4239(4), Ge1–P2 = 2.4070(4), Ge1–P3 = 2.4110(4), P1–Ge1–P2 = 86.609(14), P1–Ge1–P3 = 85.912(15), P2–Ge1–P3 = 85.412(15).

Table 2 Selected NMR data[a]

Complex	$\delta(^{31}P)$/ppm	$\delta(^{119}Sn)$[b]/ppm	$^{1}J_{^{119}SnP}$/Hz	$^{1}J_{^{207}PbP}$/Hz	Ref.
$[Sn(OTf)_2\{o\text{-}C_6H_4(PMe_2)_2\}]$ (**1**)	14.5	−690	1882	—	This work
$[Sn(OTf)_2\{o\text{-}C_6H_4(AsMe_2)_2\}]$ (**2**)	—	Not observed −886.5 (258 K)	—	—	This work
$[Sn(OTf)_2\{o\text{-}C_6H_4(PPh_2)_2\}]$ (**8**)	19.9 22.7 (258 K)	−809 −1150 (258 K)	Not observed 1550 (258 K)	—	This work
$[Sn(OTf)_2\{MeC(CH_2PPh_2)_3\}]$ (**3**)	−9.4	−834.0	1248	—	This work
$[Sn\{MeC(CH_2PPh_2)_3\}][BAr^F]_2$ (**4**)	−8.9 −6.0 (258 K)	−824.3 −843.7 (258 K)	1246 1252 (258 K)	—	This work
$[Sn\{MeC(CH_2PPh_2)_3\}][SbF_6]_2$ [c]	−11.3	−792	1279	—	12 and 13
$[Sn(OTf)\{PhP(CH_2CH_2PPh_2)_2\}][OTf]$ (**5**)	36.4, 18.5	−834	1549, 1377	—	This work
$[Sn\{PhP(CH_2CH_2PPh_2)_2\}][SbF_6]_2$ [c]	47.7, 24.9	−686	1593, 1381	—	12 and 13
$[Sn(OTf)_2\{MeC(CH_2AsMe_2)_3\}]$ (**6**)	—	Not observed −920 (258 K)	—	—	This work
$[Sn(OTf)\{P(CH_2CH_2PPh_2)_3\}][OTf]$ (**7**)	37.8, 5.5	−778.6	720, 1485	—	This work
$[Sn\{P(CH_2CH_2PPh_2)_3\}][SbF_6]_2$ [c]	36.8, 2.5	−756	702, 1487	—	12 and 13
$[Pb(OTf)_2\{o\text{-}C_6H_4(PMe_2)_2\}]$ (**9**)	74.9	—	—	1777	This work
$[Pb\{MeC(CH_2PPh_2)_3\}_2][(\mu\text{-}OTf)_3][OTf]$ (**11**)	11.6	—	—	1150	This work
$[Pb\{MeC(CH_2PPh_2)_3\}][SbF_6]_2$ [c]	13.8	—	—	1786	12 and 13
$[Pb\{MeC(CH_2PPh_2)_3\}][BAr^F]_2$ (**12**)[c]	15.8 (258 K)	—	—	1777	This work
$[Pb(OTf)_2\{P(CH_2CH_2PPh_2)_3\}]$ (**13**)	77.5, 26.1	—	—	437, 1870	This work
$[Pb\{P(CH_2CH_2PPh_2)_3\}][SbF_6]_2$ [c]	80.1, 27.5	—	—	476, 2136	12 and 13
$[Pb\{PhP(CH_2CH_2PPh_2)_2\}][SbF_6]_2$ [c]	90.2, 66.0	—	—	1836, 1863	12 and 13

[a] Spectra recorded at 298 K in MeCN unless otherwise stated. [b] Reference $SnMe_4$ ($\delta = 0$). [c] Spectrum recorded in $MeNO_2$.

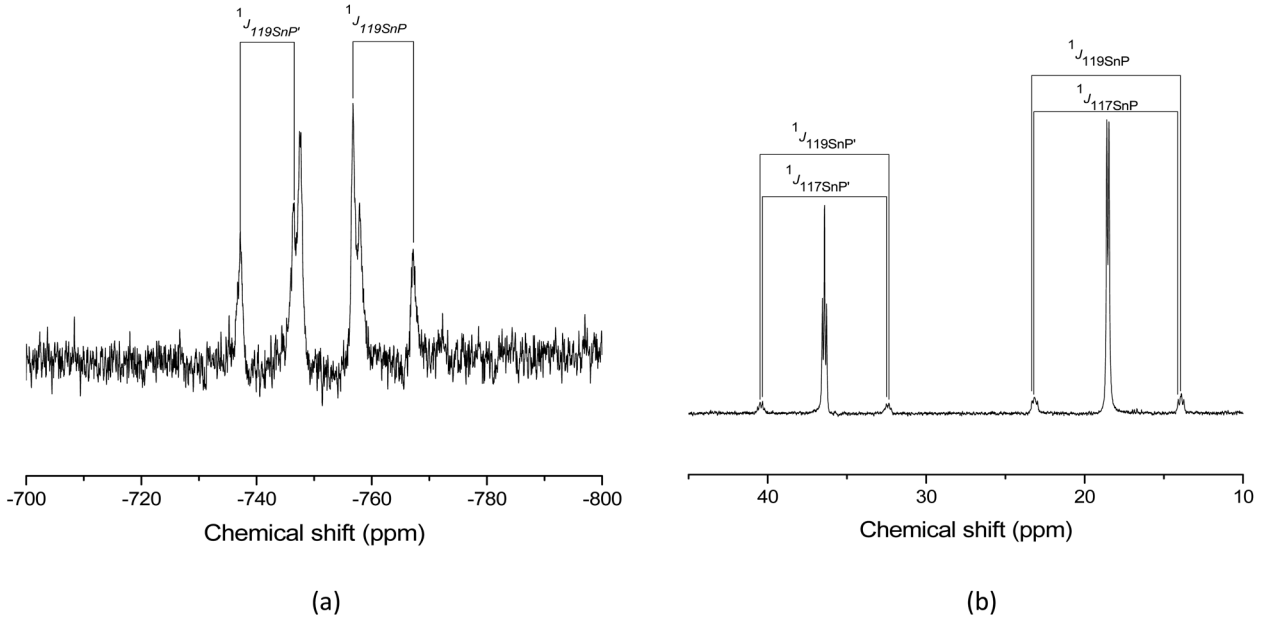

Fig. 11 (a) ^{119}Sn NMR spectrum of $[Sn(OTf)\{PhP(CH_2CH_2PPh_2)_2\}][OTf]$ (**5**) showing the $^{1}J_{^{119}SnP}$ couplings to the two distinct P atoms; (b) $^{31}P\{^{1}H\}$ NMR spectrum $[Sn(OTf)\{PhP(CH_2CH_2PPh_2)_2\}][OTf]$ (**5**) showing the $^{1}J_{^{117/119}SnP}$ and $^{1}J_{^{117/119}SnP'}$ couplings.

DFT calculations

The electronic structures of the set of dications, $[M\{MeC(CH_2PPh_2)_3\}]^{2+}$ (M = Ge, Sn, Pb), were investigated using DFT calculations as described in the Experimental section.

For the minimum energy structures located, in all cases the HOMO orbital is associated with a valence s–p hybrid orbital on the metal centre, along with ligand-centred lobes. HOMO−1 and HOMO−2 are associated with bonding interactions between the valence p orbitals on the ligand with p_x/p_y type orbitals on the group 14 centre and are approximately degenerate in energy (together with ligand-centred lobes); the HOMO orbitals are shown in Fig. 13 below. The degenerate LUMO and LUMO+1 orbitals are p_x/p_y orbitals on the metal

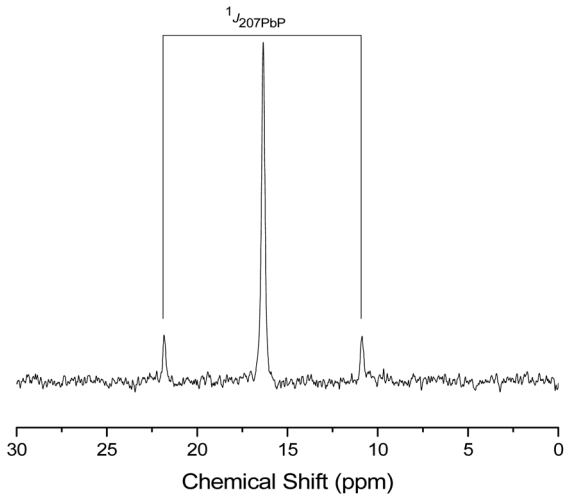

Fig. 12 The $^{31}P\{^1H\}$ NMR spectrum of $[Pb\{MeC(CH_2PPh_2)_3\}][BAr^F]_2$ (**12**) showing the $^1J_{207PbP}$ coupling.

centre (Fig. 14). The metal HOMOs on $[M\{MeC(CH_2PPh_2)_3\}]^{2+}$ are all directional with a mixture of valence s and p_z character, with germanium having the highest valence p-character (18.35%), followed by tin (13.75%) and lead (8.12%). This is consistent with the trend expected going down the group (Table 3).

The lone pair on the metal centre is *anti* to one of the P–C bonds on each arm of the tripodal phosphine ligand, this leads to a LP → P–C σ* interaction (Fig. 15). Second order perturbation theory was used to quantify the extent of this interaction (Table 3), showing that the interaction gets weaker as the group is descended, with the interaction being about half as strong in the Pb complex when compared to the Ge complex.

NBO calculations also show that the natural charge at the metal centre increases down group 14, from +0.26 for Ge to +0.76 for Sn and +0.84 for Pb. In contrast, the natural charge on the phosphorus atom decreases as the series is descended, +1.11 (M = Ge) to +0.97 (M = Sn) to +0.95 (M = Pb).

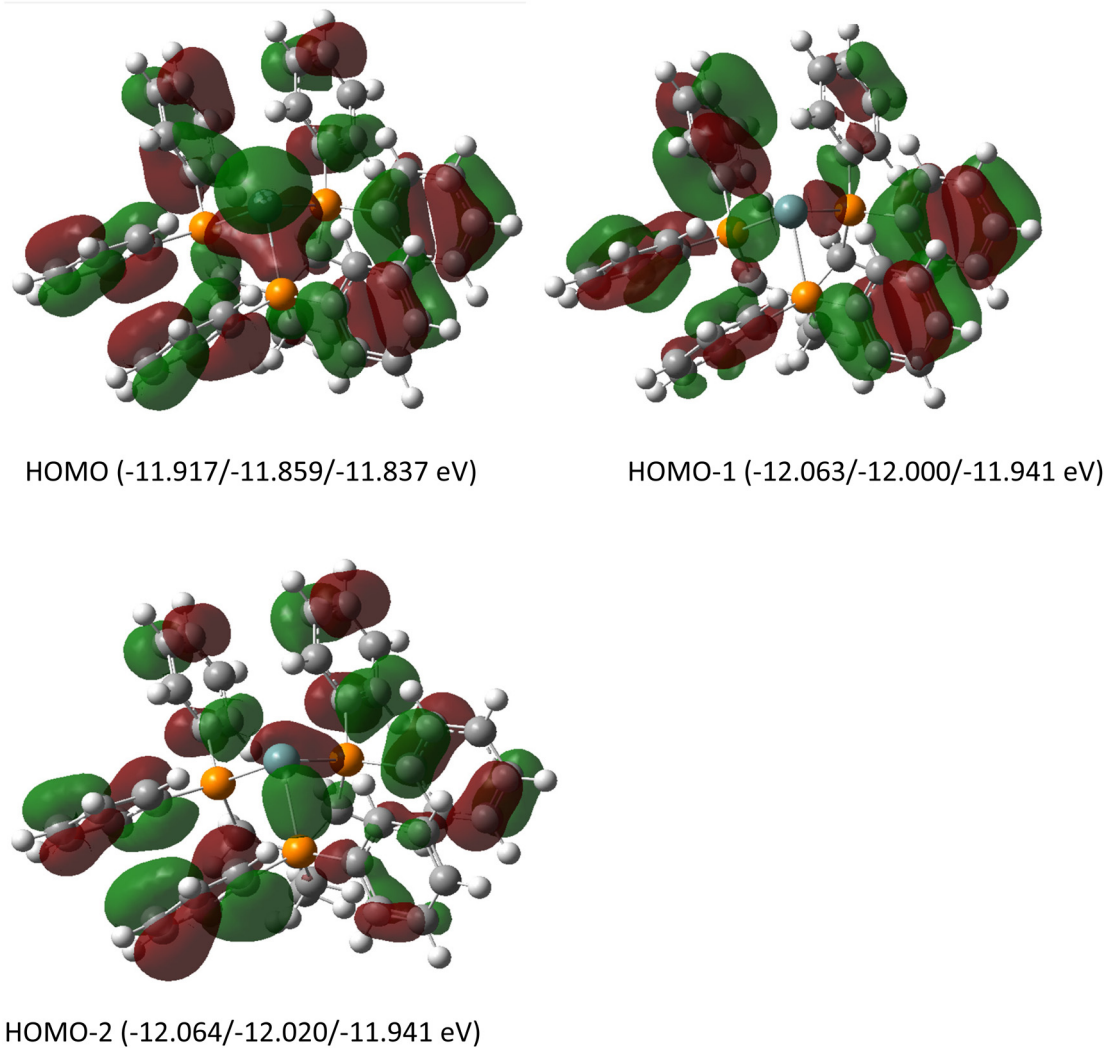

Fig. 13 Representations of the HOMO, HOMO–1 and HOMO–2 orbitals for $[Ge\{MeC(CH_2PPh_2)_3\}]^{2+}$ with the orbital energies for each complex shown in brackets (Ge/Sn/Pb).

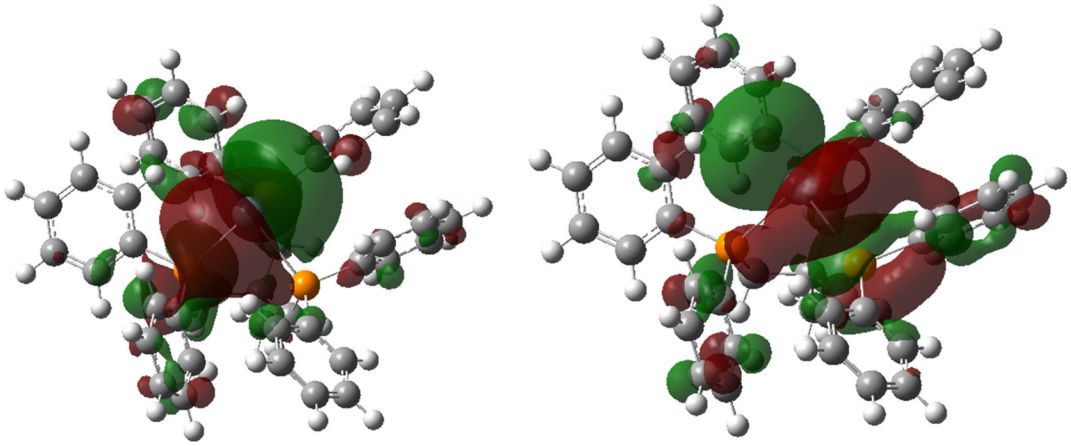

Fig. 14 Representations of the LUMO and LUMO+1 orbitals for $[Ge\{MeC(CH_2PPh_2)_3\}]^{2+}$ with the orbital energies of each complex shown in brackets (Ge/Sn/Pb).

Table 3 Summary of the orbital character and charge distributions in $[M\{MeC(CH_2PPh_2)_3\}]^{2+}$ determined from the B3LYP-D3 DFT calculations and the strength of the metal LP to P–Cσ* interactions (three of these are present in each dication)

Complex	HOMO–LUMO gap/eV	%p_z character of HOMO on M	Charge at M	Charge at P	Average metal LP to P–Cσ* interaction energy/kJ mol^{-1}
$[Ge\{MeC(CH_2PPh_2)_3\}]^{2+}$	5.17	18.35	0.26	1.11	11.36
$[Sn\{MeC(CH_2PPh_2)_3\}]^{2+}$	4.81	13.75	0.76	0.97	7.26
$[Pb\{MeC(CH_2PPh_2)_3\}]^{2+}$	4.74	8.12	0.84	0.95	5.10

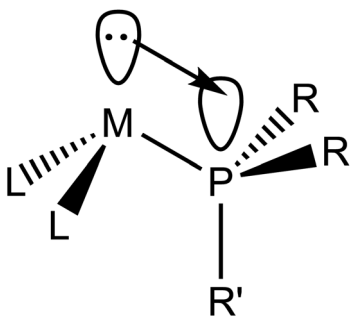

Fig. 15 Interaction between the tetral-based lone pair on the metal and the σ* orbital of the P–C bond.

Conclusions

The preparation and characterisation of a series of Sn(II) and Pb(II) triflate complexes with soft, neutral di, tri- and tetraphosphine and di- and tri-arsine ligands has been described. X-ray structural data on 12 of the complexes confirm that the structures are highly dependent upon the pnictine atom type (P *vs.* As) and denticity, and show that in the majority of cases, as well as coordinating to two or three P or As donor atoms, one or both of the OTf anions are also retained within the metal coordination sphere, giving rise to a diverse range of structural motifs. These include dicationic and monocationic monomers, weakly associated (OTf bridged) dimers, cyclic trimers or chain polymers, with the degree of association dependent upon the divalent group 14 ion. For example, $[M(OTf)_2\{o\text{-}C_6H_4(PMe_2)_2\}]$, M = Ge,[27] Sn, Pb, shows that upon changing from M = Ge to Sn to Pb, the extended structures go from dimeric to trimeric to polymeric. The triflate-bridged dimer, $[Pb\{MeC(CH_2PPh_2)_3\}_2(\mu\text{-}OTf)_3][OTf]$, undergoes anion metathesis with $Na[BAr^F]$, affording the pyramidal Pb(II) triphosphine dication, $[Pb\{MeC(CH_2PPh_2)_3\}]^{2+}$ as its BAr^F salt.

In solution the $^{19}F\{^1H\}$ NMR spectra suggest that the OTf groups are dissociated, however, the $^{31}P\{^1H\}$ NMR spectra show the expected satellite couplings to $^{117/119}Sn$ and ^{207}Pb, consistent with retention of the pnictine coordination in solution, although typically the solutions require to be cooled to reach the low temperature limiting spectra (with the exception of the tetraphosphine complexes, which are still undergoing fast exchange at 258 K). Tin-119 NMR spectra show the expected multiplet couplings to the phosphine donor groups, and the ^{119}Sn NMR shifts for the arsine complexes occur to low frequency (*ca.* 200 ppm more negative) than the corresponding phosphine species.

DFT calculations on the $[M\{MeC(CH_2PPh_2)_3\}]^{2+}$ homologues show the presence of directional HOMO in each dication, which is a mixture of valence s and p_z character, with the valence p-orbital character decreasing on going down group

14. NBO analysis also shows that the natural charge at the metal centre increases and the charge on the P centre decreases on going down group 14.

Conflicts of interest

There are no conflicts to declare.

Acknowledgements

We thank the EPSRC for support through the ADEPT Programme grant (EP/N035437/1) and through EP/R513325/1. We also thank the EPSRC National Crystallography Service for access to the X-ray diffraction facilities and Professor J. M. Dyke for helpful discussions regarding the DFT calculations.

References

1 J. Parr, in *Comprehensive Coordination Chemistry II*, ed. J. A. McCleverty and T. J. Meyer, Elsevier, 2003, vol. 3, p. 545; E. S. Claudio, H. A. Godwin and J. S. Magyar, *Prog. Inorg. Chem.*, 2003, **51**, 1; P. G. Harrison, *Comprehensive Coordination Chemistry*, Pergamon, Oxford, 1988, vol. 3, p. 183; J. R. Fulton, *Comprehensive Coordination Chemistry III*, 2021, 3.10, p. 281; *The Chemistry of Tin*, ed. P. J. Smith, Chapman & Hall, London, 1998; R. L. Davidovich, V. Stavila and K. H. Whitmire, *Coord. Chem. Rev.*, 2010, **254**, 2193; P. G. Harrison, *The Chemistry of Tin*, Blackie London, 1989.

2 W. Levason, G. Reid and W. Zhang, *Coord. Chem. Rev.*, 2011, **255**, 1319.

3 J. Burt, W. Levason and G. Reid, *Coord Chem. Rev.*, 2014, **260**, 65.

4 F. Cheng, M. F. Davis, A. L. Hector, W. Levason, G. Reid, M. Webster and W. Zhang, *Eur. J. Inorg. Chem.*, 2007, 4897; M. F. Davis, W. Levason, G. Reid, M. Webster and W. Zhang, *Dalton Trans.*, 2008, 533; M. F. Davis, W. Levason, G. Reid and M. Webster, *Dalton Trans.*, 2008, 2261; R. P. King, W. Levason and G. Reid, *Dalton Trans.*, 2021, **50**, 17751.

5 R. P. King, M. S. Woodward, J. Grigg, G. McRobbie, W. Levason and G. Reid, *Dalton Trans.*, 2021, **50**, 14400; V. K. Greenacre, R. P. King, W. Levason and G. Reid, *Dalton Trans.*, 2019, **48**, 17097.

6 F. Cheng, J. M. Dyke, F. Ferrante, A. L. Hector, W. Levason, G. Reid, M. Webster and W. Zhang, *Dalton Trans.*, 2010, **39**, 847.

7 P. A. Rupar, V. N. Staroverov, P. J. Ragogna and K. M. Baines, *J. Am. Chem. Soc.*, 2007, **129**, 15138; P. A. Rupar, V. N. Staroverov and K. M. Baines, *Science*, 2008, **322**, 1360; F. Cheng, A. L. Hector, W. Levason, G. Reid, M. Webster and W. Zhang, *Angew. Chem., Int. Ed.*, 2009, **48**, 5752; P. A. Rupar, R. Bandyopadhyay, B. F. T. Cooper, M. R. Stinchcombe, P. J. Ragogna, C. L. B. Macdonald and K. M. Baines, *Angew. Chem., Int. Ed.*, 2009, **48**, 5755; F. Cheng, A. L. Hector, W. Levason, G. Reid, M. Webster and W. Zhang, *Chem. Commun.*, 2008, 5508.

8 For examples, see: F. S. Tschernuth, F. Hanusch, T. Szilvási and S. Inoue, *Organometallics*, 2020, **39**, 4265; S. Hino, M. Brynda, A. D. Phillips and P. P. Power, *Angew. Chem., Int. Ed.*, 2004, **43**, 2655; A. P. Singh, H. W. Roesky, E. Carl, D. Stalke, J.-P. Demers and A. Lange, *J. Am. Chem. Soc.*, 2012, **134**, 4998; M. Bouška, L. Dostál, A. Růžička and R. Jambot, *Organometallics*, 2013, **32**, 1995.

9 F. Cheng, A. L. Hector, W. Levason, G. Reid, M. Webster and W. Zhang, *Inorg. Chem.*, 2010, **49**, 752.

10 R. P. King, V. K. Greenacre, W. Levason, J. M. Dyke and G. Reid, *Inorg. Chem.*, 2021, **60**, 12100.

11 C. Gurnani, A. L. Hector, E. Jager, W. Levason, D. Pugh and G. Reid, *Dalton Trans.*, 2013, **42**, 8364.

12 P. A. W. Dean, D. D. Phillips and L. Polensek, *Can. J. Chem.*, 1981, **59**, 50.

13 P. A. W. Dean, *Can. J. Chem.*, 1983, **61**, 1795.

14 A. J. Rossini, A. W. Macgregor, A. S. Smith, G. Schatte, R. W. Schurko and G. G. Briand, *Dalton Trans.*, 2013, **42**, 9533.

15 J. Burt, W. Grantham, W. Levason and G. Reid, *Dalton Trans.*, 2015, **44**, 11533.

16 R. E. H. Kuveke, L. Barwise, Y. van Ingen, K. Vashisth, N. Roberts, S. S. Chitnis, J. L. Dutton, C. D. Martin and R. L. Melen, *ACS Cent. Sci.*, 2022, **8**, 855.

17 E. P. Kyba, S. T. Liu and R. L. Harris, *Organometallics*, 1983, **2**, 1877.

18 R. D. Feltham, A. Kasenally and R. S. Nyholm, *J. Organomet. Chem.*, 1967, **7**, 285.

19 G. M. Sheldrick, *Acta Crystallogr., Sect. C: Struct. Chem.*, 2015, **71**, 3; G. M. Sheldrick, *Acta Crystallogr., Sect. A: Found. Crystallogr.*, 2008, **64**, 112; O. V. Dolomanov, L. J. Bourhis, R. J. Gildea, J. A. L. How, J. A. L. Howard and H. Puschmann, *J. Appl. Crystallogr.*, 2009, **42**, 339.

20 M. J. Frisch, G. W. Trucks, H. B. Schlegel, G. E. Scuseria, M. A. Robb, J. R. Cheeseman, G. Scalmani, V. Barone, G. A. Petersson, H. Nakatsuji, X. Li, M. Caricato, A. V. Marenich, J. Bloino, B. G. Janesko, R. Gomperts, B. Mennucci, H. P. Hratchian, J. V. Ortiz, A. F. Izmaylov, J. L. Sonnenberg, D. Williams-Young, F. Ding, F. Lipparini, F. Egidi, J. Goings, B. Peng, A. Petrone, T. Henderson, D. Ranasinghe, V. G. Zakrzewski, J. Gao, N. Rega, G. Zheng, W. Liang, M. Hada, M. Ehara, K. Toyota, R. Fukuda, J. Hasegawa, M. Ishida, T. Nakajima, Y. Honda, O. Kitao, H. Nakai, T. Vreven, K. Throssell, J. A. Montgomery, J. E. Peralta, F. Ogliaro, M. J. Bearpark, J. J. Heyd, E. N. Brothers, K. N. Kudin, V. N. Staroverov, T. A. Keith, R. Kobayashi, J. Normand, K. Raghavachari, A. P. Rendell, J. C. Burant, S. S. Iyengar, J. Tomasi, M. Cossi, J. M. Millam, M. Klene, C. Adamo, R. Cammi, J. W. Ochterski, R. L. Martin, K. Morokuma, O. Farkas, J. B. Foresman and D. J. Fox, *Gaussian 16, Revision C.01*, Gaussian, Inc., Wallingford, CT, 2016.

21 C. Lee, W. Yang and R. G. Parr, *Phys. Rev. B: Condens. Matter Mater. Phys.*, 1988, **37**, 785; S. Grimme, J. Antony, S. Ehrlich and H. Krieg, *J. Chem. Phys.*, 2010, **132**, 154104.
22 R. Krishnan, J. S. Binkley, R. Seeger and J. A. Pople, *J. Chem. Phys.*, 1980, **72**, 650.
23 W. R. Wadt and P. J. Hay, *J. Chem. Phys.*, 1985, **82**, 284.
24 M. Mantina, A. C. Chamberlin, R. Valero, C. J. Cramer and D. G. Truhlar, *J. Phys. Chem. A*, 2009, **113**, 5806.
25 J. Emsley, *The Elements*, Oxford, 1989.
26 S. H. Strauss, *Chem. Rev.*, 1993, **93**, 927.
27 R. P. King, W. Levason and G. Reid, *Dalton Trans.*, 2021, **50**, 17751.